In vitro evaluation of direct restorations utilizing short fiber-reinforced composite without coverage

Dr András Gábor Jakab

PhD Thesis

2025 Szeged

University of Szeged
Doctoral School of Clinical Medicine

In vitro evaluation of direct restorations utilizing short fiber-reinforced composite without coverage

PhD Thesis

Dr András Gábor Jakab

Supervisor:
Dr. habil. Márk Fráter, PhD, M.Sc.

2025 Szeged

Table of Contents

1. List of the publications providing the basis of, and related to the topic of the thesis

Publications providing the basis of the thesis:

Tarjányi, T.; **Jakab, A.G.**; Sámi, M.; Bali, K.; Rárosi, F.; Jarábik, M.L.; Braunitzer, G.; Palkovics, D.; Lassila, L.; Lempel, E.; et al. The Nanomechanical Performance and Water Uptake of a Flowable Short Fiber Composite: The Influence of Bulk and Layering Restorative Techniques. Polymers 2025, 17, 1553, doi:10.3390/polym17111553. (Q1)

Jakab, A.G.; Néma, V.; Molnár, J.; Alföldi, A.; Braunitzer, G.; Palkovics, D.; Lassila, L.; Garoushi, S.; Lempel, E.; Fráter, M. Crack Propensity of Different Fiber-Reinforced Direct Restorative Procedures in Deep MOD Cavities. Dental Materials 2025, S0109564125006669, doi:10.1016/j.dental.2025.06.010. (Q1, D1)

Jakab, A.G.; Palkovics, D.; T. Szabó, V.; Szabó, B.; Vincze-Bandi, E.; Braunitzer, G.; Lassila, L.; Vallittu, P.; Garoushi, S.; Fráter, M. Mechanical Performance of Extensive Restorations Made with Short Fiber-Reinforced Composites without Coverage: A Systematic Review of In Vitro Studies. Polymers 2024, 16, 590, doi:10.3390/polym16050590. (Q1)

Related publications:

Fráter, M.; Grosz, J.; **Jakab, A.;** Braunitzer, G.; Tarjányi, T.; Gulyás, G.; Bali, K.; Villa-Machado, P.A.; Garoushi, S.; Forster, A. Evaluation of Microhardness of Short Fiber-Reinforced Composites inside the Root Canal after Different Light Curing Methods – An in Vitro Study. Journal of the Mechanical Behavior of Biomedical Materials 2024, 150, 106324, doi:10.1016/j.jmbbm.2023.106324.

Volom, A.; Vincze-Bandi, E.; Sáry, T.; Alleman, D.; Forster, A.; **Jakab, A.;** Braunitzer, G.; Garoushi, S.; Fráter, M. Fatigue Performance of Endodontically Treated Molars Reinforced with Different Fiber Systems. Clin Oral Invest 2023, 27, 3211–3220, doi:10.1007/s00784-023-04934-2.

2. List of Abbreviations

- RBC: resin based composite
- PFC: particulate filler composite
- MOD: mesio-occluso-distal
- SFRC: short fiber-reinforced composite
- FRC: fiber-reinforced composite
- Semi-IPN: semi-interpenetrating polymer network
- ANOVA: analysis of variance
- DSCF: Dwass-Steel-Critchlow-Fligner
- SEM: Scanning electron microscope

3. Introduction

One of the fundamental goals of restorative dentistry is to restore both the function and aesthetics of the dentition by replacing missing hard dental tissues. Such interventions are most often required when the tooth structure has been compromised due to caries or trauma; however, restorative needs may also arise from various forms of non-carious tissue loss. These include chemical erosion, mechanical wear caused by foreign objects (abrasion), wear from opposing teeth (attrition), and structural loss from occlusal overloading or parafunctional habits (abfraction) [1,2]. In recent years, the demand for restorative treatment has also been driven by the increasing aesthetic expectations of patients; however, the primary reason for restorative treatments remains the restoration of tooth structure lost due to caries [3]. Depending on the case, restoration may be fabricated extraorally (indirect restoration) with the involvement of a dental technician, or intraorally (direct restoration) by the dentist during a single visit [4,5]. Among the available options for restoring cavities caused by caries, direct restorations are most commonly employed and professionally accepted. The shared interest of both patients and practitioners in minimally invasive approaches that preserve tooth structure, combined with the growing aesthetic demands of patients and the need to reinforce structurally compromised teeth, highlights the need for a restorative material that meets these requirements. Especially in modern societies, where patients are increasingly exposed to elevated levels of physical and psychological stress and therefore restorations must withstand excessive bite forces (such as those caused by bruxism), the reinforcement of the remaining tooth structure is of key importance [6]. For permanent teeth, resin based composites (RBCs) have become the most favored and widely used in recent years [7–9]. A 2012 publication estimated the annual number of composite fillings at around 260 million [10]. By 2015, this number had reached approximately 800 million, with 80% applied in posterior and 20% in anterior teeth, based on the quantity of resin material sold worldwide [11].

3.1 Mechanical properties of particulate filler composites

The widespread adoption of RBCs is due not only to their tooth-colored appearance and capacity for conservative preparation, but also to their continuous advancements in adhesive and filler technologies [12]. These materials typically consist of four key components: an organic polymer matrix, inorganic filler particles, a coupling agent, and an initiator-accelerator system [13]. The organic matrix usually contains dimethacrylate monomers such as bisphenol-A glycidyl dimethacrylate, urethane dimethacrylate, and triethylene glycol dimethacrylate, each offering specific advantages in viscosity and polymerization kinetics [14]. Inorganic fillers—

commonly silica, zirconia, or glass ceramics—vary in particle size and morphology and significantly influence mechanical strength, polishability, and wear resistance [12]. To ensure chemical integration between the organic and inorganic phases, filler particles are coated with organosilane coupling agents. These facilitate covalent bonding between the methacrylate groups and filler surfaces. Polymerization is triggered via light, chemical, or dual-curing mechanisms, forming a crosslinked polymer network. The most commonly used RBC materials share similar physical properties, such as elastic modulus ~10–20 GPa, tensile strength ~40–60 MPa, flexural strength ~130–190 MPa, fracture toughness ~1.2–1.43 $MPa \cdot m^{0.5}$, Vickers hardness ~55–105 [15,16]. While these properties make RBCs highly suitable restorative materials for direct restorative purposes, however, they still present certain limitations. Dentin is a hydrated, collagen-rich vital tissue that underlies the enamel and forms the bulk of the tooth structure. It is an elastic and resilient tissue, with an elastic modulus ranging from 14–20 GPa, a tensile strength of ~105 MPa, and Vickers hardness of ~60 [17]. Its fracture toughness typically ranges between 2.5 and 3.5 $MPa \cdot m^{0.5}$, depending on factors such as measurement method, location within the tooth (coronal vs. root dentin), and hydration state [18]. The first main limitation of conventional particulate filler composites (PFCs) is that these materials fall short in terms of fracture toughness compared to dentin (this will be addressed in a separate section in 3.2.2. in the thesis). Although modern RBCs are strong and wear-resistant, they remain brittle and are vulnerable to crack initiation and propagation, especially in restorations with high cavity volume and reduced cusp support [19–23]. The second main limitation of RBCs is their polymerization shrinkage which occurs as the resin matrix converts from a monomeric to a polymeric state [24,25]. This volumetric shrinkage generates contraction stresses that can compromise the adhesive interface, leading to marginal gap formation, microleakage, and eventually secondary caries [24,26] The latter is discussed under 3.4.

3.2 Fracture Toughness of composite materials

Beyond polymerization shrinkage, one of the most critical mechanical shortcomings of PFCs is their inherently low fracture toughness. Fracture toughness is a material's intrinsic ability to resist crack propagation once a flaw has been initiated [27,28]. In the context of restorative dentistry, this property plays a pivotal role in the long-term survival of restorations, particularly in high-stress areas such as the posterior dentition, where restorations are subjected to cyclic loading, lateral forces, and occasional traumatic stress events [11]. As already mentioned above, the fracture toughness of dentin is significantly higher than that of typical PFCs [18,29]. This disparity reveals a fundamental mismatch when composite materials are used to replace lost

dentin in deep cavities. The inability of PFCs to adequately mimic the damage-tolerant behavior of dentin becomes a critical issue in restorations that are exposed to functional loading over extended periods. Once a crack forms in the PFC material, it often progresses unimpeded due to the brittle nature of the matrix and the absence of mechanisms to dissipate energy. This is particularly evident in larger MOD restorations or in endodontically treated teeth, where significant loss of tooth structure and internal line angles create areas of concentrated stress [30,31]. From a restorative perspective, it becomes evident that mimicking the biomechanical characteristics of the dentin—especially its fracture-arresting behavior—is crucial for achieving long-term success in the posterior region [17]. This recognition has driven the development of restorative strategies and materials that seek not only to replace missing hard tissue anatomically, but also to replicate its mechanical function.

3.3 Factors influencing the success of composite restorations

As described above, direct RBC restorations have inherent limitations that affect their long-term success. A systematic review by Manhart and colleagues found annual failure rates ranging from 1% to 3% for posterior RBCs, with survival outcomes ranging between 70% and 98% after observation periods of 8 to 22 years [32]. Importantly, the extent of the restoration has a direct correlation with its clinical longevity: while small, single-surface restorations demonstrate relatively low failure rates, the risk of failure increases substantially with larger restorations [33]. For example, restorations involving four or more surfaces may exhibit annual failure rates of 9.43%, primarily due to secondary caries and fractures [34]. These complications are particularly common in deep mesio-occluso-distal (MOD) restorations, where extensive loss of tooth structure subjects the remaining walls and the restorative material to significant biomechanical stress [35].

3.4 Volumetric shrinkage of resin-based composites

The polymerization of RBCs results in a volume reduction ranging from less than 1% to as much as 6%, depending on the composition and curing conditions [24,25]. Polymerization shrinkage occurs as the distance between monomers decreases, when weak van der Waals forces between monomers are replaced by covalent bonds. During this reaction, the viscosity of the resin material increases, and it gradually loses its ability to flow. Following gelation and during the vitrification phase, the material undergoes a transition to a solid-like state. Prior to the vitrification process, RBCs exhibit the capacity to flow and partially release tensile stresses induced by the contraction of the RBC bonded to the tooth. However, as the material undergoes

vitrification, it becomes more rigid and its elastic properties increase [24]. Consequently, the factors limiting polymerization shrinkage generate residual shrinkage stresses [24,36–41]. These stresses may manifest in various clinical symptoms, such as marginal staining, secondary caries, and pulpal inflammation, due to the penetration of saliva, bacteria, and other irritants through the debonded interface [42–47]. Postoperative hypersensitivity, resulting from fluid flow in the exposed dentinal tubules, is associated with cracks caused by cuspal deflection or gap formation at the restoration-tooth interface, often due to bending or insufficient bond strength [48,49]. Gap formation can lead to fluid movement in the dentin tubules, and the flow of dentinal fluid through the adhesive may create fluid-filled regions, contributing to the degradation of adhesives [42,50–53]. Cuspal deflection is a common biomechanical phenomenon characterized by the linear movement of the cusp tips in a restored tooth, resulting from the interaction between the polymerization shrinkage stress of the RBC and the compliance of the cavity wall (determined by the continuity, thickness, as well as the length of the remaining walls) [42,54]. RBC restorations have been reported to exhibit cuspal deflections ranging from approximately 10 μm to 40 μm, with variations depending on the measurement method, tooth type, and cavity size [55]. Cuspal deflection is influenced by two main categories of biomechanical factors. The first category includes geometrical and material factors, such as the volume of the cavity (primarily its width and depth), the compliance of the cavity wall, the polymerization shrinkage of the RBC, and the creep and compliance of the cured RBC and tooth [54,56–61]. As shown in a research on cuspal deflection, deep MOD cavities in the posterior region exhibit the greatest degree of cuspal deflection due to the absence of marginal ridges [30]. The loss of both marginal ridges creates a mechanical issue [31,62]. According to a previous study larger restorations were associated with lower stress levels at the restoration and tooth/restoration interface but increased stresses within the tooth [63]. Cavity size and configuration (C-factor) also influence the extent of cuspal deflection, with the highest deflection values observed in MOD cavities. It has been demonstrated that preparing standardized MOD cavities results in an average loss of 63% in relative cuspal stiffness due to the loss of marginal ridge integrity [62,64], with a concomitant loss of approximately 54% in fracture strength [65,66]. The anticipated number of fatigue fractures is proportional to the magnitude of cuspal flexure [64–66]. An *in vitro* study dealing with different sized of MOD cavities suggest that in such clinical situations, a depth of 5 mm is critical, as material-related disadvantages (such as suboptimal fracture toughness) begin to manifest at this point [67]. The second category includes clinical factors, such as the use of a liner, the filling technique (bulk filling versus incremental filling), the type of restorative approach (direct versus indirect), and

the use of light-curing methods that influence the polymerization rate [54,61,68–73]. Numerous potential solutions can be found in the literature to decrease cuspal deflection and, consequently, reduce the formation and propagation of cracks. These methods include the incremental layering technique, whereby the RBC is applied in horizontal or oblique increments with a maximum thickness of 2 mm, aimed to reduce polymerization shrinkage-induced stress [68,74]. However, Bicalho and colleagues managed to show that layering does not reduce polymerization induced cuspal flexure [39]. Furthermore, layering methods are time-consuming and complex technique, leading to the development of special bulk-fill RBCs. These RBCs utilize stress modulators and highly reactive photoinitiators incorporated into the material to reduce polymerization stress [68]. An approach to reducing cuspal deflection is the application of a flowable RBC as an intermediate layer, which serves as an alternative to the "elastic cavity wall" concept proposed for filled adhesives. According to this approach, the stress generated by the next layer of higher modulus RBC is absorbed by an elastic intermediate layer, thereby reducing the stress at the tooth/restoration interface, which is clinically manifested by a reduction in cuspal deflection [61,69,75,76]. Glass-ionomer cements and resin-modified glass-ionomer cements have also been suggested as liners to provide a stress-buffering layer that aids in stress reduction [77,78]. Additionally, ultra-high molecular weight polyethylene fiber (Ribbond-Ultra THM; Ribbond Inc., Seattle WA, USA), in the form of leno weave, could alter the stress dynamics at the restoration/adhesive resin interface by creating multiple stress paths along the fibers, redistributing the load to the intact parts of the tooth and away from the bonded surfaces [79]. Further advancements resulted in the introduction of short fiber-reinforced composite (SFRC) materials, which, due to its key role in this thesis, will be discussed in a following, separate section.

3.5 The introduction of fiber-reinforced materials

In cases requiring the replacement of a substantial volume of dentin, the use of PFC restorative materials is far from ideal. One of the core issues lies in the fundamental difference between the microstructure of composite materials and that of dentin [28]. While dentin consists of collagen fibers embedded in a hydroxyapatite matrix, conventional composites are composed of inorganic filler particles dispersed in a resin matrix. It is evident that restoring large volumes of dentin calls for a material that mimics dentin not only in terms of mechanical properties but also in structural composition. Among the mechanical characteristics critical to the long-term success of a restoration, fracture toughness plays a particularly decisive role [83,84]. Therefore, an ideal dentin-replacing material should demonstrate a fracture toughness comparable to that

of natural dentin. Although fiber-reinforced dental materials date back to the 1960s, a paste-consistency SFRC truly suitable for direct dentin replacement – EverX Posterior (GC Europe, Leuven, Belgium) – only became available in 2013.

3.5.1 Composition and mechanical properties of SFRC materials

SFRC materials consist of a resin matrix—referred to in this case as a semi-interpenetrating polymer network (semi-IPN)—and inorganic filler particles, similar to any other PFC [85]. What distinguishes SFRCs is the incorporation of randomly oriented short glass fibers. The reinforcing effect of the short glass fibers is influenced by several key factors. One of the most critical is the aspect ratio—the length-to-diameter ratio of the fibers—which determines whether the fibers are subjected to tensile stress [28,86]. The fibers can contribute to reinforcement only if they are adequately tensioned, which occurs when their aspect ratio exceeds 30 [86]. Beyond aspect ratio, the quality of the bond between the semi-IPN matrix and the glass fibers plays a crucial role [86–88]. The effectiveness of reinforcement is also shaped by the orientation of the fibers within the matrix, as well as the overall fiber content of the material [89]. These parameters collectively determine the material's ability to absorb stress and resist crack propagation under functional load.

The reinforcing capacity of glass fibers in SFRC is only reliable when their aspect ratio (length/diameter) falls within the range of approximately 30 to 94 [28,86]. This ratio determines the minimum fiber length necessary for effective stress transfer from the resin matrix to the fibers, allowing them to bear tensile loads and thereby contribute to crack prevention within the matrix. If the aspect ratio is below the critical threshold of 30, the fibers act as inert fillers and do not provide meaningful reinforcement. As discussed previously, fracture toughness is among the most important mechanical parameters influencing the longevity of restorations. In this respect, EverX Posterior, a paste-consistency SFRC, has demonstrated significant improvement over PFCs. Studies have reported fracture toughness values in the range of 2.4–2.6 $MPa \cdot m^{0.5}$ for EverX Posterior, which closely approximates the behavior of natural dentin and far exceeds that of typical PFCs [90,91]. An additional benefit of the glass fiber component in SFRC is its positive effect on polymerization depth. The dispersed fibers serve not only as reinforcement but also as conduits for light transmission, scattering the curing light through the material and allowing effective polymerization up to depths of 4 to 5 mm. This bulk-curing capability is of particular clinical value in deep cavities, where incremental layering of conventional composites would otherwise be required [91]. To further improve handling characteristics, particularly in large restorations or anatomically complex regions such as occlusal boxes or root

canals, a flowable version of SFRC (EverX Flow; GC Europe) was introduced in 2019. Unlike traditional flowable composites, which generally compromise mechanical integrity for improved adaptability, EverX Flow maintains or even surpasses the performance of its paste-like predecessor. Its fracture toughness has been reported at 2.8 $MPa \cdot m^{0.5}$, outperforming EverX Posterior [88]. This improvement is attributed to key differences in fiber morphology and content. While EverX Posterior contains short glass fibers in the millimeter range, EverX Flow incorporates micro-scale fibers, which allows for a denser fiber network. Consequently, the fiber volume content is significantly higher in EverX Flow (25 vol%) compared to EverX Posterior (9 vol%). Despite the difference in fiber size, both variants exceed the critical length threshold, ensuring their effectiveness in reinforcing the material, mitigating internal stress, and arresting crack propagation.

3.5.2 The use of SFRC materials without coverage

The paste-consistency EverX Posterior is recommended by the manufacturer for the replacement of large volumes of dentin, with subsequent coverage by another direct (most commonly by PFC) or indirect restorative material. Although the incorporation of millimeter-scale glass fibers improves several key properties of the material, as discussed earlier, it still lacks certain essential characteristics required for its use without coverage. Excessive wear and surface roughness—both of which may contribute to increased plaque retention—have been commonly associated with earlier generations of SFRC materials. However, with the introduction of the newer flowable SFRC, these issues appear to be resolved. This is due to the micrometer-sized fibers incorporated in the flowable version. EverX Flow had a significantly lower wear value after 15,000 chewing simulation cycles than conventional PFCs, and it did not exhibit a coarse surface after the test. This SFRC material fulfilled the American Dental Association's criterion for wear [88]. In an earlier study, after 100,000 cycles of brushing simulation, it was found that SFRC had a similar wear and surface roughness to that of PFC [92]. During the polishing of these materials, the fibers on the surface suffer microfractures; thus, they can be polished together with the resin matrix [88]. With these recent findings it has been shown that these SFRC materials are suitable to use them not just as a dentin substitute, but rather for complete restorations. A usual concern regarding these materials is their water absorption after restoration. Lassila et al. compared the water absorption of flowable SFRC to conventional bulk-fill PFC. After 36 days, the material's water absorption was the second best (0.5 wt%), while other regular bulk-fill composite materials had much higher values (Estelite Bulk Fill Flow 1.1 wt%) [88]. As the previously mentioned shortcomings of the material have

been resolved with the introduction of the new flowable SFRC, researchers were able to investigate its biomechanical effects in various configurations — both when covered with different thicknesses of conventional PFC and when used without any PFC coverage. In our recently published review article, which serves as one of the basis of the present thesis, we collected the available studies that investigated the use of SFRC materials without any PFC coverage. Eight of the studies included in the systematic review compared an uncovered, plain SFRC group to a bi-layered SFRC + PFC group as well [85,93–99]. In all eight publications, the uncovered SFRC performed better than the bi-layered group. Lassila et al. compared EverX Flow covered by 2 mm PFC on the occlusal surface to uncovered flowable SFRC in posterior crown restorations. They found that the uncovered group performed significantly better than the covered ones [99]. In another publication, they compared posterior crown restorations made with a flowable SFRC (EverX Flow) core covered by PFC layers of different thicknesses (0.5, 1, 1.5, 2). They also included an uncovered, plain SFRC group and a fully PFC-made group. Regression analysis showed that by decreasing the thickness of the PFC layer, the load-bearing capacity increased. The uncovered, plain SFRC group had a significantly higher load-bearing capacity than all other tested groups [95]. Garoushi et al. tested direct onlay restorations made of plain PFC, SFRC + PFC, and plain SFRC [85]. Similarly to the crown restorations, the uncovered SFRC group exhibited the highest load-bearing capacity, which was significantly higher than that of the control PFC group.

In the above-mentioned systematic review, fifteen of the included articles also investigated fracture pattern. Thirteen reported a favorable pattern for the SFRC groups [85,93–98,102–106]. Bielic et al. found that both the SFRC and the control group had favorable fracture patterns [97]. In another publication, they reported that the control group showed a slightly more favorable fracture pattern, but the difference from the SFRC group was not statistically significant [107]. Despite the manufacturer's original recommendation to use SFRCs exclusively as a substitute for missing dentin in direct and indirect restorations while avoiding contact with the oral environment, the study's findings suggest that employing SFRCs without surface coverage in various simulated clinical scenarios yielded satisfactory outcomes in terms of restoration fracture behavior. This might improve the clinical performance of extensive direct composite restorations; however, it is necessary to conduct clinical trials to obtain more reliable and conclusive findings.

3.6 Objectives

Building on recent findings, flowable short fiber-reinforced composite (SFRC) materials have shown potential for use as direct restorative materials without the need for an overlying particulate filler composite (PFC) layer. This could significantly improve the structural integrity of restorations. However, for a material to be applied in the oral cavity without coverage, it must satisfy specific mechanical and functional criteria. This thesis presents a comprehensive summary and critical evaluation of two in vitro studies that examined distinct but related aspects of SFRC-based restorative strategies. The first study investigated whether various modern direct restorative techniques—such as bulk-fill SFRC without occlusal coverage, or in combination with an elastic base (with or without polyethylene fibers)—would influence crack formation in comparison to traditional layered PFC restorations.

The null hypotheses tested in that study were:

1. There would be no differences in the number of cracks immediately after the restorative procedure among the tested restorations.
2. There would be no differences in the number of cracks one week after the restoration.
3. There would be no differences in the number of cracks five weeks after the restoration among the groups.
4. There would be no significant change in crack formation within the same group over the three time points during the five-week observation period.

The second study focused on the nanomechanical surface characteristics and water uptake behavior of flowable SFRC under different application protocols. Through nanoindentation and bulk compressive creep testing, the study assessed the material's suitability for clinical use with or without surface coverage.

The null hypotheses for the second study were:

5. There would be no significant differences in surface hardness among the tested materials.
6. There would be no significant differences in bulk compressive creep between the different application techniques (bulk vs. layered).
7. The water uptake and degradation of the SFRC material would not differ significantly from those of the conventional PFC.

4. Materials and methods

The *in vitro* study involving human extracted teeth was approved by the Ethics Committee of the University of Szeged and the Medical Research Council of Hungary (BM/23566–1/2023), and it adhered to the principles outlined in the Declaration of Helsinki.

4.1 Specimen acquisition for the study on crack propensity

A total of 100 mandibular third molars, extracted for orthodontic purposes, were included in the study. The selected teeth exhibited consistent coronal dimensions, with orovestibular diameters ranging from 9 to 10 mm, mesiodistal diameters ranging from 10 to 11 mm, and crown heights (measured from the cemento-enamel junction) ranging from 6 to 8 mm. Throughout the study, the samples were preserved in 0.9% saline solution at room temperature. All teeth were used within 6 months of extraction.

4.2 Specimen preparation for the study on crack propensity

Class II MOD cavities were prepared in all teeth included in the study. In alignment with previous research, the cavity dimensions were standardized to a depth of 5 mm and a wall thickness of 2.5 mm for both the oral and vestibular walls [67,108,109]. The preparation protocol [110] was carried out as follows: a round end parallel diamond bur (881.31.014 FG – Brasseler USA Dental, Savannah, GA, USA) was used, initially positioned at the midpoint of the occlusal surface, calculated by dividing the distance between the buccal and lingual cusp tips. During the preparation, the wall thickness at the cavity base was continuously monitored with a digital caliper (Mitutoyo Corp., Kawasaki, Japan) to ensure a uniform 2.5 mm thickness. The cavity walls were aligned parallel to the tooth axis. The depth of the cavity was assessed using a 15 UNC periodontal probe (Hu-Friedy Mfg. Co., Chicago, USA), measuring from the corresponding cusp tip while ensuring full contact with the cavity wall. The final cavity was a single, continuous structure, with the proximal box having identical width and depth to the occlusal portion. Cavosurface margins were prepared perpendicular to the tooth surface upon completion of the cavity preparation. Following cavity preparation, all teeth were thoroughly examined for cracks using D-Light Pro (GC Europe) in "detection mode”, at 4.3x magnification. Any teeth exhibiting pre-existing enamel cracks were excluded from the sample set and replaced with crack-free specimens following the MOD cavity preparation. Ultimately, 100 third molars with prepared MOD cavities were included in the study and randomly allocated into five groups (n = 20/group).

4.3 Restorative procedures for the study on crack propensity

All teeth received the same adhesive treatment as follows. A Tofflemire matrix (1101 C 0.035, KerrHawe, Bioggio, Switzerland) was applied, and the enamel surrounding the cavity was etched with 37 % phosphoric acid for 15 s, followed by rinsing with water. After drying the cavity, a one-step self-etch adhesive system (G-Premio Bond, GC Europe) was applied in accordance with the manufacturer's instructions. The adhesive was light-cured for 60 s using an Optilux 501 quartz-tungsten-halogen light-curing unit (Kerr Corp., Orange, CA, USA). The average radiant exitance of the curing unit, measured with a digital radiometer (Bluephase Meter II, Ivoclar Vivadent, Solna, Sweden), was 820 ± 40 mW/cm². Following the restoration of each fifth tooth, the radiant exitance was evaluated with a radiometer to guarantee that all RBCs were subjected to an identical irradiation. The class II cavities were first converted to class I using the centripetal technique by building up the proximal walls. In the control group (Group 5), a conventional PFC material (G-aenial A′CHORD, GC Europe) was used, while in the remaining groups (Groups 1–4), SFRC material (EverX Flow Dentin Shade, GC Europe) was employed for this purpose. The handling of the packable materials (G-aenial A′CHORD and EverX Posterior) was facilitated using an Optrasculpt Pad (Ivoclar, Schaan, Liechtenstein) compaction tool, which was thinly coated with modeling resin (Modeling Liquid, GC Europe, Leuven, Belgium). The cavities were then restored in one of the below listed ways:

Group 1 (n = 20): The cavities were restored using a single 4 mm thick bulk layer of flowable SFRC (EverX Flow Bulk Shade, GC Europe), shaped according to the dentin anatomy, leaving a 1 mm space for the occlusal covering. The bulk SFRC layer was light-cured for 40 s and subsequently covered with a flowable SFRC layer (EverX Flow Dentin Shade). The occlusal layer was then light-cured for 20 s.

Group 2 (n = 20): Initially, a thin layer (maximum 0.5 mm) of conventional flowable PFC (G-aenial Hiflo, GC Europe) was applied to cover the occlusopulpal cavity wall and light-cured for 40 s. From this point, the cavities were restored in the same manner as described for Group 1.

Group 3 (n = 20): Similar to Group 2, a thin layer (maximum 0.5 mm) of conventional flowable PFC (G-aenial Hiflo) was used to cover the occlusopulpal cavity wall. Before polymerization, additionally, a piece of ultra-high molecular weight polyethylene fiber (Ribbond-Ultra THM) was placed over the occlusopulpal surface and embedded in the flowable PFC, which was then light-cured for 40 s. The cavities were subsequently restored as described in Group 1.

Group 4 (hybrid SFRC restoration, n = 20): The cavity was partially filled with flowable SFRC (EverX Flow Bulk Shade), up to half of its depth. Next, packable SFRC (EverX Posterior) was placed and condensed into the center of the flowable SFRC (using snowplow technique), ensuring that the flowable material covered all areas of the axial walls, leaving 1 mm for the occlusal coverage. This hybrid SFRC layer was light-cured for 40 s, followed by the application of a flowable SFRC layer (EverX Flow Dentin Shade) to cover the surface. The occlusal layer was light-cured for 20 s.

Group 5 (control group, n = 20): The cavities were restored using conventional PFC (G-aenial A′CHORD) with an oblique layering technique. Each layer was approximately 2 mm thick, with the deeper layers light-cured for 40 s, and the superficial layers for 20 s. The restorations were finished using a fine-grit diamond bur (FG 7406–018, Jet Diamonds, Ft. Worth, TX, USA, and FG 249-F012, Horico, Berlin, Germany) and polished with aluminum oxide polishers (OneGloss PS Midi, Shofu Dental GmbH, Ratingen, Germany). The restored teeth were stored in physiological saline solution until the experimental procedures began. The study groups, application methods, and the investigated materials are summarized in Table 1.

Table 1. *Study groups, materials and application methods*

Group		Application method	Used materials
Group 1	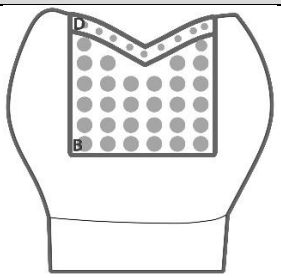	SFRC flow (bulk shade) used with bulk-fill method. Coronally 1 mm thick layer of SFRC flow (dentin shade)	EverX Flow, bulk and dentin shade
Group 2	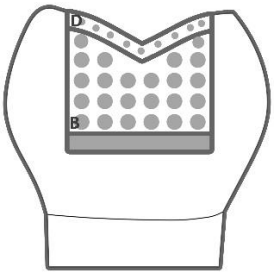	Flowable conventional resin composite base (U shade) + bulk-fill SFRC flow bulk shade + coronally 1 mm SFRC flow (dentin shade)	Essentia HiFlo as flowable base, then EverX Flow bulk and dentin shade
Group 3	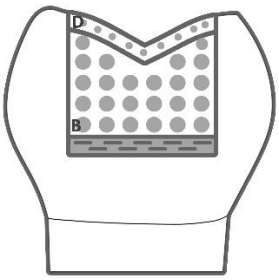	Polyethylene fibers embedded in the flowable composite base + bulk-fill SFRC flow (bulk shade) + coronally 1 mm SFRC flow (dentin shade)	Ribbond fibers + Essentia HiFlo as flowable base, then EverX Flow bulk and dentin shade
Group 4	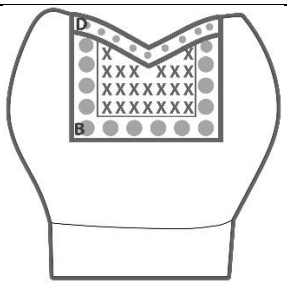	SFRC flow (bulk shade) and packable SFRC using snow plaw technique. Coronally 1 mm SFRC flow dentin shade.	EverX Flow (bulk and dentin shade) + EverX Posterior (bulk shade)
Group 5 (control)	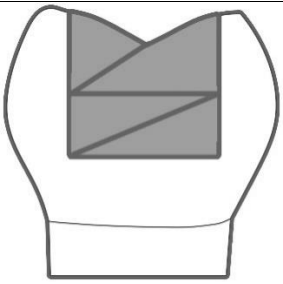	2 mm thick oblique layers of conventional packable resin composite	G-ænial A'chord (A2 shade)

4.4 Screening for cracks in the restored teeth

Crack screening was performed using D-Light Pro (GC Europe) at 4.3x magnification under transillumination in "detection mode", following a protocol requiring agreement between two examiners, as outlined by Néma et al. [110]. The light source was applied in multiple positions over the external tooth surface for 1–2 min to ensure no cracks were overlooked. In this study, only cracks measuring 2 mm or longer were classified as shrinkage-induced cracks (Figure 1). Crack lengths were measured using a 15 UNC periodontal probe (Hu-Friedy Mfg. Co., Chicago, USA) positioned parallel to the remaining coronal surface of the tooth adjacent to the crack. Both the presence and the orientation (vertical or horizontal) of the cracks were recorded. The teeth were examined for cracks at three time points: at three time points: immediately after polymerization, one week later, and five weeks later. Between the sessions, the teeth were stored in physiological saline solution.

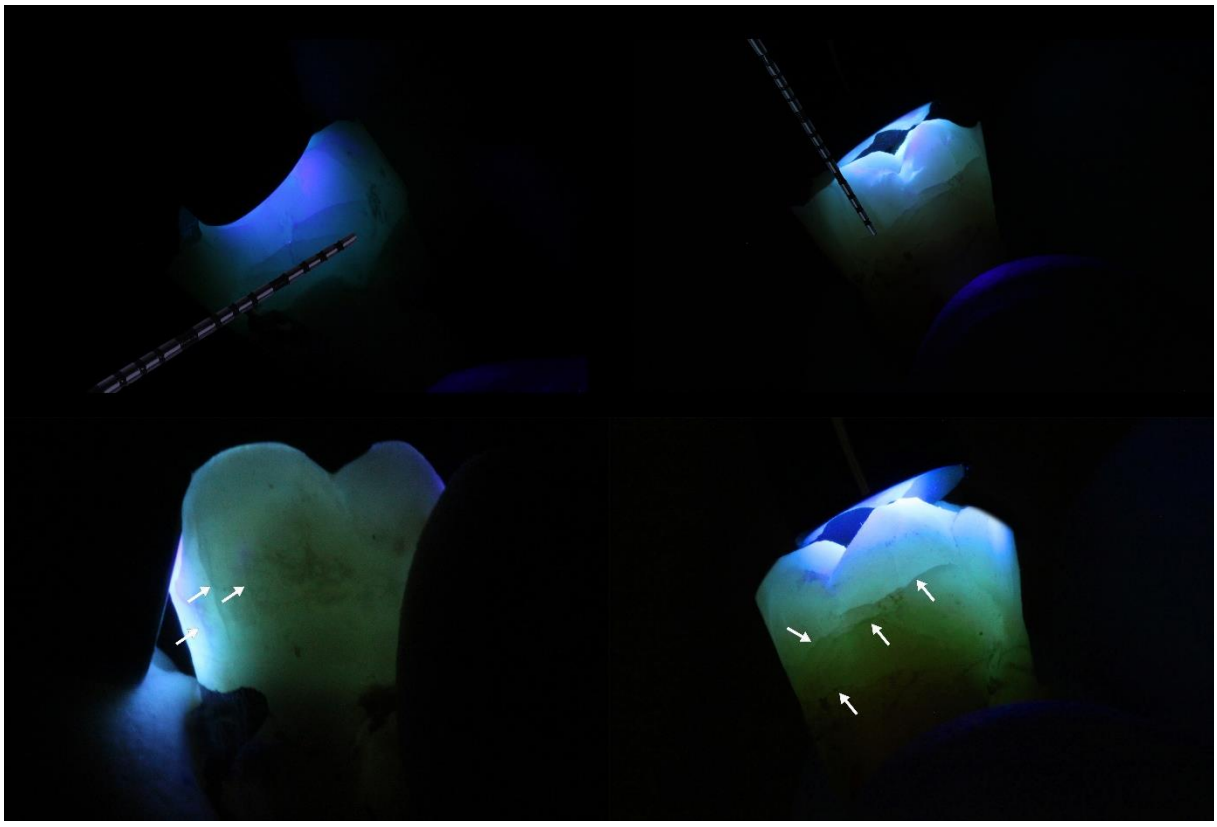

Figure 1. *The images illustrate the detection of vertical and horizontal crack formation (indicated by arrows) observed during the polymerization process. A 15 UNC periodontal probe was used under transillumination to measure the length of the detected cracks. Both the orientation and length of cracks were documented*

4.5 Statistical analysis for the study on crack propensity

For the statistical analyses, Jamovi 2.3.28 was used. Descriptive statistics were calculated to summarize the distribution of crack counts (total, vertical, and horizontal) for each group at each time point following the restorative procedure. For each crack type, the mean, median, standard deviation, minimum, and maximum were calculated. For all hypothesis tests involving the five groups, a significance level of $p < 0.01$ was applied, as adjusted by the Bonferroni correction to control for multiple comparisons. The assumption of normality was not met in all cases, thus non-parametric tests (Kruskal-Wallis and Friedman analysis of variance; ANOVA) were applied to analyze differences between and within groups. The primary analysis assessed differences in crack counts between groups at specific time points: immediately after the restorative procedures, and then one week and five weeks later. The Kruskal-Wallis test was used to determine significant differences in total, vertical, and horizontal crack counts across groups at each time point. For significant Kruskal-Wallis results, Dwass-Steel-Critchlow-Fligner (DSCF) post-hoc pairwise comparisons were conducted to identify specific group differences (level of significance: $p < 0.05$). For the post-hoc power analyses, G*Power 3.1 (Universitat ¨ Düsseldorf, Germany) was used. The secondary analysis examined changes in crack counts over time within each group. Friedman's ANOVA was used to evaluate temporal changes in total, vertical, and horizontal crack counts within each group. Where significant differences were observed, Durbin-Conover post-hoc pairwise comparisons were conducted to detect differences between specific time points within each group (level of significance: $p < 0.05$).

4.6 Specimen preparation for the study on nanomechanical performance and water uptake of SFRC

This study examined three types of resin composites, a flowable bulk-shade SFRC (everX Flow, GC Europe), a bulk-fill PFC composite (SDR flow+, Dentsply Sirona), and a conventional PFC composite (G-aenial Posterior, GC Europe), each applied using different techniques.

Eighteen standard-size composite specimens were fabricated for each group using a 5 × 5 × 5 mm metallic mold (n = 18/group). The specimens were prepared with different materials and application strategies according to five study groups (Table 2).

Group 1 (control group): three consecutive layers of a packable conventional PFC (G-aenial Posterior) were applied in 2 mm, 2 mm, and 1 mm thick layers, respectively. Each layer was photopolymerized for 20 s according to the manufacturers' instructions using a high-performance hand-held curing lamp (D-Light Pro). The average power density of the

photopolymerization unit was 940 ± 20.8 mW/cm^2. This was measured with a digital radiometer (Jetlite light tester, J. Morita USA Inc. Irvine, CA, USA) before performing the restorations.

Group 2 (layered SFRC): three consecutive layers of a flowable SFRC were applied in the same manner as in Group 1. Each layer was photopolymerized for 20 s.

Group 3 (bulk SFRC): the same flowable SFRC material used in Group 2 was applied in a single 5 mm thick layer (bulk-fill technique). Each specimen was photopolymerized for 20s.

Group 4 (bulk PFC): a flowable bulk-fill PFC material was used in the same way as described for Group 3. The specimens were photopolymerized for 20 s.

Group 5 (bi-structure): two consecutive layers (2 mm each) of SFRC were applied, with each layer photopolymerized for 20 s. The SFRC was then covered with a 1 mm layer of PFC, as described in Group 1.

Table 2. *Experimental groups categorized by composite material and application technique.*

Group	Material	Application Technique
1 (Control)	PFC	Layered (2–2–1 mm)
2	SFRC	Layered (2–2–1 mm)
3	SFRC	Bulk
4	Bulk-fill PFC	Bulk
5	SFRC + PFC	Layered (2–2–1 mm)

After photopolymerization, the specimens were stored under dry conditions at room temperature to allow for post-polymerization curing for several days. Each specimen was then polished using silicon carbide (SiC) abrasive papers with progressively finer grits. Polishing began with P1500 grit until the surface was smooth, followed by P2000 and P2500 grits until surface scratches were eliminated and an appropriate surface roughness was achieved. In total, at least a 100 μm surface layer was removed during the polishing process. After polishing, the specimens were mounted onto a stainless-steel specimen holder using an optical adhesive diluted with acetone. The adhesive mixture was applied to the surface of the specimen holder, and the specimens were pressed continuously until the adhesive dried to ensure proper adhesion.

4.7 Nanoindentation protocol

The nanomechanical surface properties of the composite specimens were tested using the IND-1500 nanoindenter (Semilab, Budapest, Hungary) one week after the specimens were fabricated and dry-stored at room temperature. A Berkovich diamond tip (Semilab, Budapest, Hungary)

was used for the nanoindentation tests (Figure 2). A fresh area correction function for the tip was pre-measured on fused silica, and the compliance of the measurement device was set to 0.0003 μm/mN. The measurements and analysis followed the ISO 14577 standard [111]. The device operated in force control mode with a maximum force set to 20 mN, an initial contact force of 0.15 mN, and a hold at maximum force for 1 s. Each specimen underwent 19 nanoindentations at 40 μm intervals between indents. Each group consisted of 18 specimens, which were randomly divided into three subgroups: 6 specimens for topside measurements, 6 for side measurements, and 6 for bottom measure-ments. This resulted in a total of 1710 nanoindentations (19 indents × 18 specimens × 5 groups) on the dry specimens. The Poisson's ratio for the composite materials was set to 0.27 for the analysis. The analysis was conducted using the method of Oliver and Pharr [112].

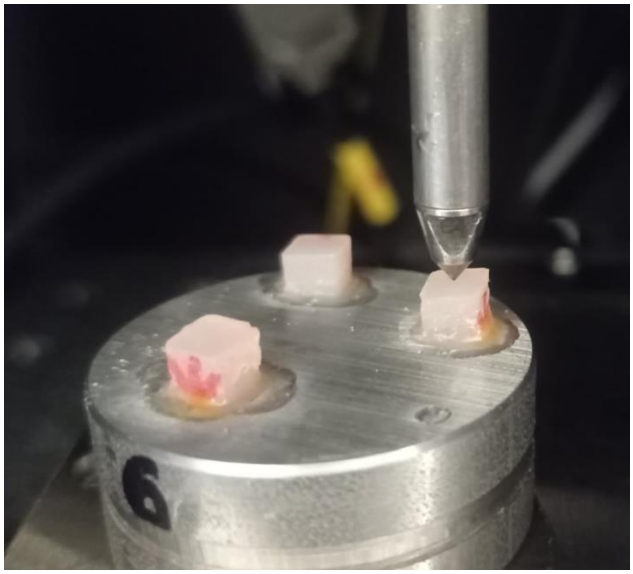

Figure 2. *Nanoindentation measurement setup. The composite specimens were polymerized on the top side with the curing lamp positioned accordingly. The arrow on the specimens indicates the direction of polymerization, pointing toward the bottom surface.*

4.8 Nanoindentation creep investigation

Additional creep measurements were conducted on the six specimens from each group following the initial static nanoindentation test. Each specimen was subjected to 10 creep measurements at 50 μm intervals using the IND-1500 nanoindenter, equipped with a Berkovich diamond tip (50 nm radius of curvature), at room temperature. The loading force for the creep measurements was maintained at a constant 25 mN over a 300 s period, during which 300 data points were collected. The standard linear model was used to evaluate the creep behavior by fitting the time-dependent penetration curve. This model consists of a Hooke body connected

in series to a Kelvin–Voigt model, which comprises a Hooke and a Newton body connected in parallel, as illustrated in Figure 3.

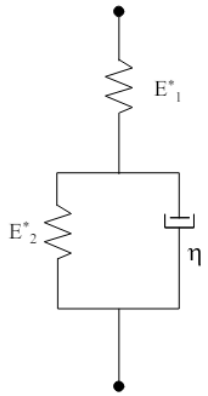

Figure 3. *Schematic representation of the standard linear viscoelastic model.*

The analytical solution for the displacement in the case of constant loading (creep) is represented by the following equation:

$$h^2(t) = \frac{\pi}{2} F \cdot \cot\alpha \left[\frac{1}{E_1^*} + \frac{1}{E_2^*} \left(1 - e^{-\frac{E_2^* t}{\eta}} \right) \right]$$

where F represents the applied loading force, α is the angle of the conical indenter tip, and E_1^*, E_2^*, and η are the combined modulus of elasticity and viscosity values of the standard linear model. The least squares method was applied to the measured $h(t)$ time-dependent displacement curves to fit the standard linear model. The specimen modulus value can then be calculated from the fitted E_1^*, E_2^* combined modulus values using the following formula:

$$\frac{1}{E^*} = \frac{1 - \nu_s^2}{E_s} + \frac{1 - \nu_i^2}{E_i}$$

where E_s is the specimen modulus, E_i is the indenter tip modulus (diamond $E_i = 1050$ GPa), ν_s is the Poisson's ratio of the specimen, and ν_i is the Poisson's ratio of the indenter tip (diamond $\nu_i = 0.07$).

Additionally, the total displacement during the creep measurements was calculated by recording the displacement at 300 s and subtracting the depth at the start of the measurement. This value is referred to as creep depth in the following sections.

4.9. Water degradation and water uptake

After the initial set of nanoindentation tests, the specimens were measured for their dimensions and weight using a micrometer and an analytical balance (Ohaus Pa224c, with an accuracy of 0.1 mg).The nanoindentation creep test was conducted both before and after a 30-day water-aging period at a laboratory room temperature of 24 °C. The static nanoindentation measurements were repeated on the six top side specimens following the water-aging period. The results from the two tests were compared statistically to assess the effect of water degradation.

The dry weight of each specimen was recorded immediately after preparation. During the water-aging period, weights were measured at 1, 2, 3, 4, 10, 14, 28, and 30 days (m_w) using the analytical balance. The absorbed water mass per unit volume uptake was calculated using the following formula:

$$\varphi = \frac{m_w - m_0}{V},$$

where m is the mass measured on the actual day, m_0 is the initial mass at day 0, and V is the volume of the composite specimen.

4.10 Surface morphology and characterization

Secondary electron images were taken using a Hitachi S-4700 (Hitachi High-Technologies Corporation, Tokio, Japan) field emission cathode scanning electron microscope (FESEM). The surfaces of the specimens were coated with a few- nanometer-thin electrically conducting golden layer for the elimination of surface charging. To facilitate the identification of the imprints, extra nanoindentations were per-formed at a greater loading force to find the imprints.

4.11 Statistical analysis for the study on nanomechanical performance and water uptake of SFRC

Statistical analysis was performed using IBM SPSS Statistics, version 23 (IBM Corp., Armonk, NY, USA). The normality of the data was assessed using the Shapiro–Wilk test, and the homogeneity of variances was evaluated with Levene's test. For group comparisons, a one-way ANOVA was conducted, followed by Bonferroni's post hoc test to identify significant differences between individual groups. Mean values and standard deviations were calculated and reported for each group. A significance level of $p < 0.05$ was considered statistically significant.

Additionally, the creep behavior of the materials was analyzed using a curve fitting approach based on the least squares method to accurately model time-dependent deformation. This allowed for the extraction of parameters that describe the viscoelastic response over time. All analyses were performed with a minimum of six specimens per group to ensure sufficient statistical power.

5. Results

5.1. Results of the first study: Crack propensity of different fiber-reinforced direct restorative procedures in deep MOD cavities

Regarding the crack propensity of different fiber-reinforced direct restorative procedures in deep MOD cavities, immediately following the restorative procedure, there was no significant difference in the total crack counts (horizontal + vertical) across the tested groups ($\chi^2 = 7.43$, $p = 0.115$). Likewise, no statistically significant differences were found across the groups when horizontal ($\chi^2 = 1.99$, $p = 0.737$) and vertical ($\chi^2 = 12.74$, $p = 0.013$) crack counts were analyzed separately (Figs. 4–6). One week after the restorative procedure, the total crack counts varied across the five groups significantly ($\chi^2 = 24.60$, $p < 0.001$). Group 5 had the highest mean number of cracks, while Group 1 exhibited the lowest. The DSCF post-hoc pairwise comparisons revealed significant differences between several groups. Specifically, Group 5 (control group) had a significantly higher number of cracks compared to Group 1 ($p < 0.001$), Group 2 ($p = 0.023$), and Group 3 ($p = 0.003$). Additionally, Group 4 had significantly more cracks than Group 1 ($p = 0.024$). These results suggest that Group 5 (control group) suffered the most cracking at one week, while Group 1 consistently showed fewer cracks. The presence of statistically significant differences highlights the variability in crack formation among the different groups shortly after the restorative procedure. The descriptive statistics are shown in Table 3. As for the vertical crack counts, these also varied significantly among the five groups one week after the restorative procedures ($\chi^2 = 22.20$, $p < 0.001$). Again, Group 5 (control group) exhibited the highest number of cracks, with a mean of 2.90, a median of 3.00, and a standard deviation of 0.91, ranging from 1 to 5 cracks. The lowest number of cracks was observed in Group 3, with a mean of 1.15 (median = 1.00, SD = 1.23). The DSCF post-hoc pairwise comparisons, revealed significant differences in vertical crack counts between several groups. Group 5 (control group) demonstrated a significantly higher number of vertical cracks compared to Group 1 ($p < 0.001$), Group 3 ($p < 0.001$), and Group 4 ($p = 0.004$) (Table 3).

Regarding the horizontal crack counts, these also varied significantly among the five groups one week after the restorative procedures ($\chi^2 = 16.01$, $p = 0.003$). Groups 4 and 5 (control group) exhibited the highest number of cracks. In contrast, the lowest number of cracks was observed in Group 2. The DSCF post-hoc pairwise comparisons revealed significant differences in horizontal crack counts between several groups. Group 4 had a significantly higher number of horizontal cracks compared to Group 1 ($p = 0.029$) and Group 2 ($p = 0.016$) (Table 3).

Table 3. *Total, vertical, and horizontal crack counts across the groups 1 week after restoration.*

	Group	Mean	Median	SD	Minimum	Maximum
Total crack counts	Group 1	3.55	4.00	1.54	1	6
	Group 2	4.00	4.00	2.62	0	8
	Group 3	4.15	4.00	1.53	1	7
	Group 4	5.10	5.00	1.37	2	7
	Group 5 (control)	6.70	6.50	2.13	3	11
Vertical crack counts	Group 1	1.20	1.00	0.89	0	3
	Group 2	1.70	1.00	1.84	0	6
	Group 3	1.15	1.00	1.23	0	4
	Group 4	1.30	1.00	1.38	0	4
	Group 5 (control)	2.90	3.00	0.91	1	5
Horizontal crack counts	Group 1	2.35	2.50	1.57	0	5
	Group 2	2.30	2.50	1.49	0	5
	Group 3	3.00	3.00	1.21	0	5
	Group 4	3.80	4.00	1.28	1	7
	Group 5 (control)	3.80	3.50	1.77	1	6

When examining the total crack counts 5 weeks after the restorative procedure, the observed pattern was quite similar to what had been seen at the 1-week examination. There was a significant variability across the groups ($\chi^2 = 20.45$, $p < 0.001$). The DSCF post-hoc pairwise comparisons revealed significant differences in total crack counts between several groups. Group 5 (control group) demonstrated a significantly higher number of total cracks compared to Group 1 ($p = 0.001$) and Group 3 ($p = 0.016$). Additionally, Group 1 showed a significantly lower number of cracks than Group 4 ($p = 0.014$). The difference between Group 5 (control group) and Group 2 approached significance ($p = 0.055$). The descriptive statistics are shown in Table 4. Vertical crack counts continued to vary across the five groups at 5 weeks ($\chi^2 = 18.91$, $p < 0.001$). Group 5 (control group) exhibited the highest mean number of vertical cracks. In

contrast, Group 3 displayed the lowest mean number of cracks. The DSCF post-hoc pairwise comparisons revealed significant differences in vertical crack counts between several groups. Group 5 (control group) demonstrated a significantly higher number of vertical cracks compared to Group 1 ($p < 0.001$), Group 2 ($p = 0.023$), and Group 3 ($p = 0.002$) (Table 4). As for the horizontal crack counts at 5 weeks, these showed some variation across the five groups, but this did not reach the level of statistical significance ($\chi^2 = 10.33$, $p = 0.035$). Group 4 exhibited the highest mean number of horizontal cracks, and Group 1 showed the lowest mean number of cracks (Table 4). Due to the lack of significant variance among groups, no post-hoc comparisons were performed.

Table 4. *Total, vertical, and horizontal crack counts across the groups 5 week after restoration*

	Group	Mean	Median	SD	Minimum	Maximum
Total crack counts	Group 1	4.40	5.00	1.82	1	8
	Group 2	5.15	5.50	2.96	0	10
	Group 3	5.10	5.50	2.00	1	8
	Group 4	6.50	6.00	2.04	3	11
	Group 5 (control)	8.20	8.00	3.12	3	14
Vertical crack counts	Group 1	1.65	1.00	1.04	0	3
	Group 2	2.05	2.00	1.76	0	6
	Group 3	1.60	1.50	1.39	0	4
	Group 4	2.25	2.00	1.86	0	6
	Group 5 (control)	4.05	3.50	2.14	1	9
Horizontal crack counts	Group 1	2.75	3.00	1.71	0	5
	Group 2	3.10	3.50	1.74	0	6
	Group 3	3.50	3.50	1.61	0	7
	Group 4	4.25	4.00	1.37	1	7
	Group 5 (control)	4.15	4.50	1.98	1	7

The significant differences from all the above analyses, along with significance levels, effect sizes and estimated statistical power are summarized in Table 5. As for the analysis of crack counts within individual groups over time, we conducted a Friedman's ANOVA for the total crack count, as well as for the vertical and horizontal cracks. In every case, the analysis showed significant variance, indicating that crack counts in each group changed significantly over time (Figs. 4–6). According to the Durbin-Conover post-hoc pairwise comparisons, this also meant that, with one exception, there was a significant change between each time point in every group.

The sole exception was the horizontal crack count in Group 2, which did not change significantly during the first week.

Table 5. *Significant intergroup differences 1 week (T1) and 5 weeks (T2) after the restorative procedures. Pairwise comparisons. Level of significance: p<0.05*

Time point	Crack count	Comparison	p	Cohen's d	Power
T1	Total	Group 5 vs Group 1	< 0.001	1.69	1.00
		Group 5 vs Group 2	0.023	1.13	0.94
		Group 5 vs Group 3	0.003	1.38	0.99
		Group 4 vs Group 1	0.024	1.06	0.91
	Vertical	Group 5 vs Group 1	< 0.001	1.89	1.00
		Group 5 vs Group 3	< 0.001	1.62	1.00
		Group 5 vs Group 4	0.004	1.37	0.99
	Horizontal	Group 4 vs Group 1	0.029	1.01	0.88
		Group 4 vs Group 2	0.016	1.08	0.91
T2	Total	Group 5 vs Group 1	0.001	1.49	0.99
		Group 5 vs Group 3	0.016	1.18	0.95
		Group 4 vs Group 1	0.014	1.09	0.92
	Vertical	Group 5 vs Group 1	< 0.001	1.43	0.99
		Group 5 vs Group 2	0.023	1.02	0.88
		Group 5 vs Group 3	0.002	1.36	0.99
	Horizontal	No post-hoc comparisons were made due to the lack of significant variance among groups.			

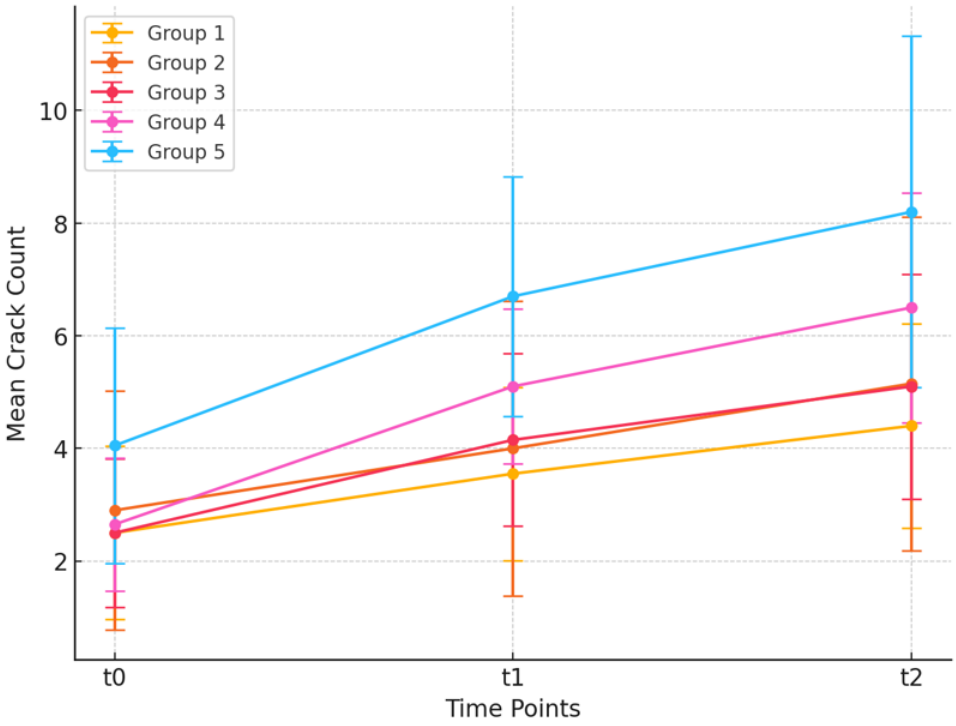

Figure 4. *Mean total crack counts across time (t0, immediately after photo-polymerization; t1, after soaking in water for one week; t2, after soaking in water for five weeks) by group. Values are shown as mean±SD.*

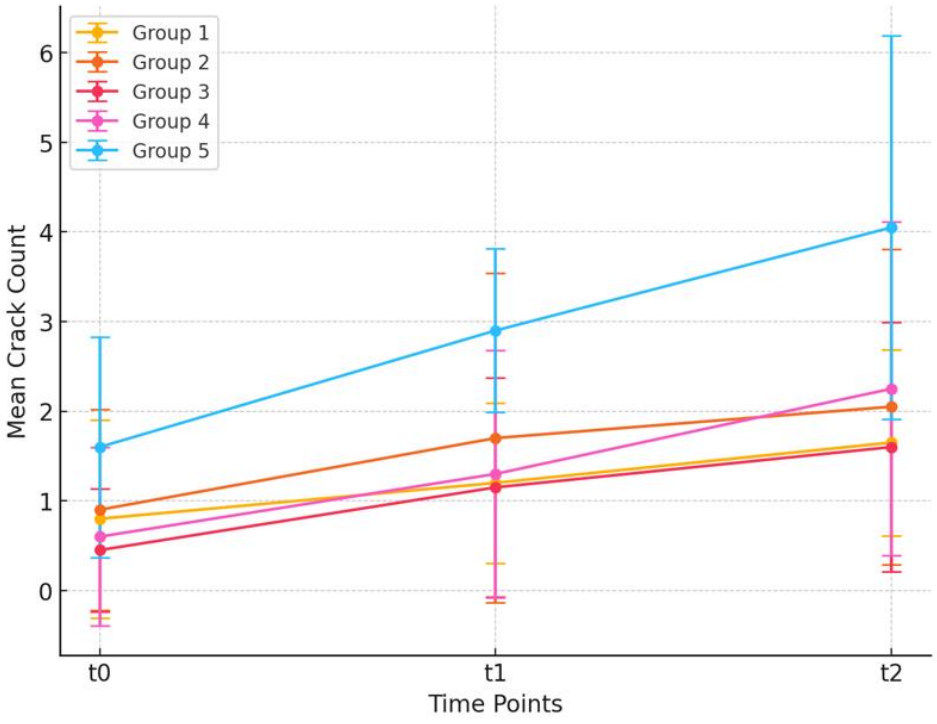

Figure 5. *Mean vertical crack counts across time (t0, immediately after photo-polymerization; t1, after soaking in water for one week; t2, after soaking in water for five weeks) by group. Values are shown as mean±SD.*

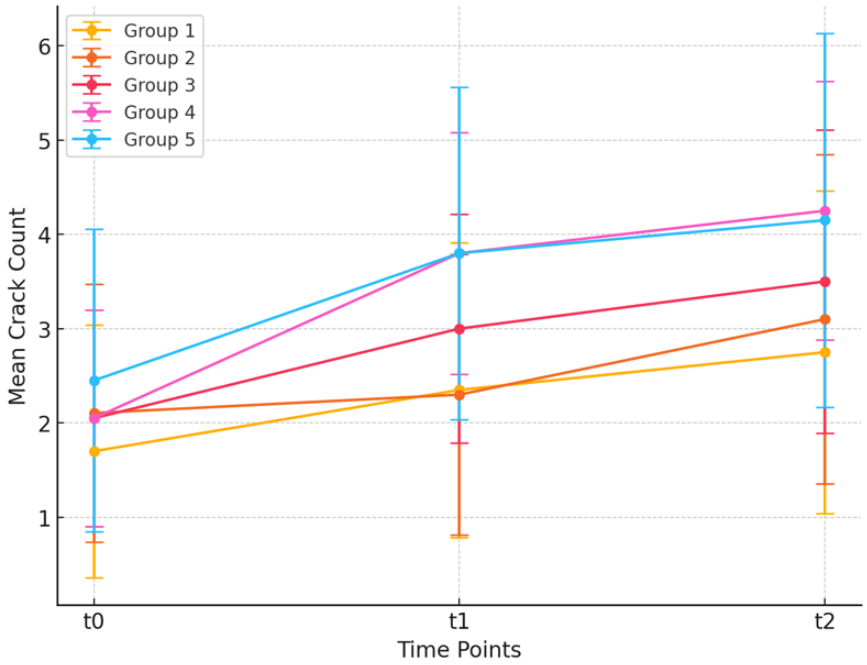

Figure 6. *Mean horizontal crack counts across time (t0, immediately after photo-polymerization; t1, after soaking in water for one week; t2, after soaking in water for five weeks) by group. Values are shown as mean±SD.*

The summarized results of the Friedman ANOVA for each group are presented in Table 6.

Table 6. *Results of the Friedman ANOVA. Level of significance: p<0.01*

Group 1			
	χ^2	df	p
Vertical	15.6	2	< 0.001
Horizontal	23.3	2	< 0.001
Total	29.5	2	< 0.001
Group 2			
Vertical	17.2	2	< 0.001
Horizontal	19.0	2	< 0.001
Total	29.5	2	< 0.001
Group 3			
Vertical	20.6	2	< 0.001
Horizontal	26.1	2	< 0.001
Total	35.4	2	< 0.001
Group 4			
Vertical	21.5	2	< 0.001
Horizontal	31.6	2	< 0.001
Total	34.8	2	< 0.001
Group 5			
Vertical	30.1	2	< 0.001
Horizontal	28.0	2	< 0.001
Total	34.6	2	< 0.001

5.2 Results of the second study: The Nanomechanical Performance and Water Uptake of a Flowable Short Fiber Composite: The Influence of Bulk and Layering Restorative Techniques

5.2.1 Static nanoindentation

The static nanoindentation measurements were conducted on the top and bottom layers of the composite specimens. Additionally, the top surface of the composite blocks was measured both before (dry) and after water storage (wet). The ANOVA revealed significant differences in the mean hardness values between the composite groups (illustrated in Figure 7). In the top layer before water storage, the bulk PFC group (Group 4) exhibited a statistically significantly lower mean hardness value compared to the other groups ($p < 0.05$), and the control group (layered PFC, Group 1) also showed a difference compared to the bulk SFRC specimens (Group 3) ($p = 0.028$). After water storage, the top layer was remeasured on the same specimens, and the Bonferroni post hoc results indicated that a significant difference remained for the bulk PFC group (Group 4) compared to the other groups ($p < 0.05$), except for the control group (layered PFC, Group 1). However, the control group (layered PFC, Group 1) showed a significant difference in mean hardness compared to the layered SFRC group (Group 2) and the bi-structure group (Group 5) (both $p < 0.001$) after water storage. For the bottom layer, a similar trend was observed as in the top layer before water storage, with the post hoc results showing that the bulk PFC group (Group 4) had a statistically significantly lower mean hardness value compared to the other groups ($p < 0.05$).

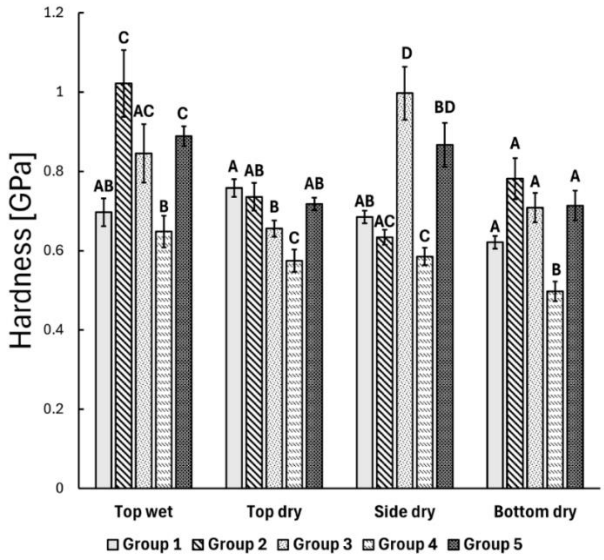

Figure 7. *The mean hardness of each composite group measured by the static nanoindentation method. The error bar shows the standard error of the mean. Identical alphabetic letters (A–D) indicate no significant difference, while different letters denote a significant difference.*

5.2.2 Creep nanoindentation

During the creep measurements, the penetration depth (displacement) was continuously recorded over 300 s under a fixed 10 mN load. The standard linear model, as outlined in the methods, was used to fit the displacement curve with three parameters: E1, E2 and η. The E1 modulus describes the initial elastic behavior at the first measured time point, which relates to the stiffness of the material, while the E2 and η parameters characterize the time-dependent behavior of the material, indicating a delayed or retarded response. Measurements were conducted on the top layer of each group, both before and after storing the specimens in distilled water. The results are shown in Figures 8–10.

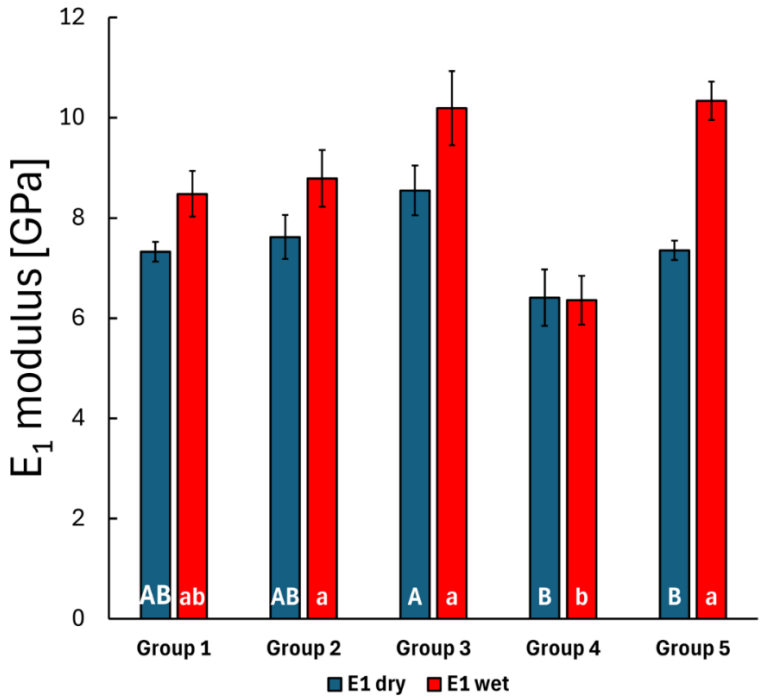

Figure 8. *The mean E_1-fitted parameter of the measured creep curves for the composite groups before and after water storage, with error bars representing the standard error of the mean. Lowercase alphabetic letters (a,b) refer to the dry groups; uppercase alphabetic letters (A,B) refer to the wet groups. Identical letters (regardless of case) indicate no significant difference, whereas different letters (irrespective of case) denote a significant difference.*

The Bonferroni post hoc test results indicated a significant difference in the mean E1 modulus value between the bulk SFRC specimens (Group 3) and the bulk PFC specimens (Group 4) ($p = 0.005$), while no significant difference was observed for this parameter among the other groups. This slightly changes after storing the specimens in water, as the mean E1 modulus differs significantly in the case of the bulk PFC (Group 4) to the layered SFRC (Group 2) ($p = 0.031$) specimens and to the bulk SFRC specimens (Group 3) ($p < 0.001$). The E2 and η

parameters showed significant changes after the 30-day water treatment. Before water treatment, the E2 parameter exhibited significant differences between the layered SFRC (Group 2) and the bulk SFRC (Group 3) group ($p < 0.001$), between the layered SFRC (Group 2) and the bulk PFC (Group 4) group ($p = 0.011$), and also between the bulk SFRC (Group 3) and the bi-structure (Group 5) group ($p = 0.001$). The mentioned difference between the layered SFRC (Group 2) and the bulk PFC (Group 4) specimens remained consistent after water treatment ($p < 0.001$), and the bulk SFRC (Group 3) versus the bulk PFC (Group 4) specimens also showed a significant difference ($p < 0.001$). The viscosity parameter for the pre-treated specimens showed a significant difference between the bulk SFRC (Group 3) and the bulk PFC (Group 4) specimens according to the Bonferroni post hoc test ($p = 0.035$). Post water storage, the time-dependent behavior described by the viscosity parameter varied significantly, with the bulk PFC (Group 4) group differing from all other groups ($p < 0.05$), and the control group (layered PFC, Group 1) also differed from the bi-structure group (Group 5) ($p < 0.001$). The mean modulus and viscosity parameters were compared before and after the 30-day water-aging period using a t-test. The E1 modulus showed a significant difference after the water treatment in the case of the control group (Group 1, $p = 0.009$) and the bi-structure group (Group 5, $p < 0.001$). The E2 modulus and η viscosity parameters showed a significant difference across all groups after the water treatment. Overall, water treatment significantly affected the time-dependent behavior, with notable differences in the retarded modulus and viscosity values.

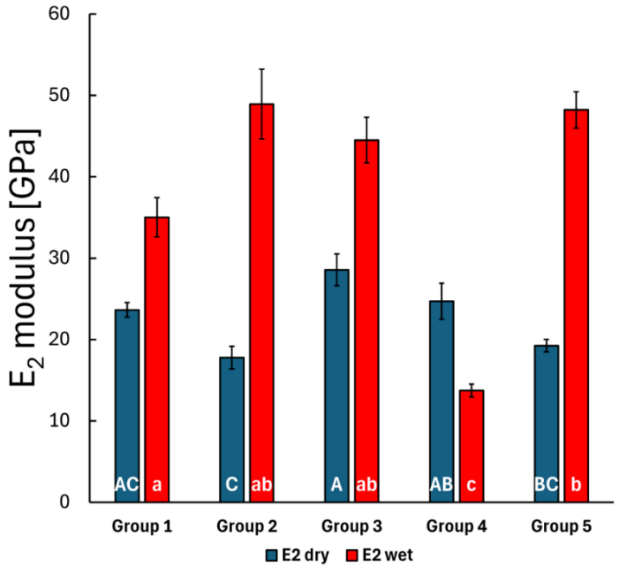

Figure 9. *The mean E_2-fitted parameter of the measured creep curves for the composite groups before and after water storage, with error bars representing the standard error of the mean. Lowercase alphabetic letters (a–c) refer to the dry groups; uppercase alphabetic letters (A–C) refer to the wet groups. Identical letters (regardless of case) indicate no significant difference, whereas different letters (irrespective of case) denote a significant difference.*

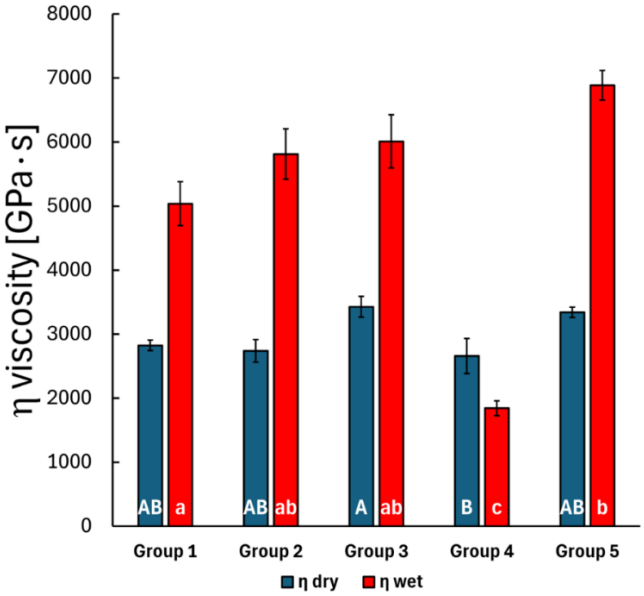

Figure 10. *The mean η-fitted parameter of the measured creep curves for the composite groups before and after water treatment, with error bars representing the standard error of the mean. Lowercase alphabetic letters (a–c) refer to the dry groups; uppercase alphabetic letters (A–C) refer to the wet groups. Identical letters (regardless of case) indicate no significant difference, whereas different letters (irrespective of case) denote a significant difference.*

The total penetration depth was recorded during the 300 s creep measurement, and the absolute depth penetration (creep depth, see Figure 11) was calculated by subtracting the initial penetration (displacement at time zero, the initial contact) from the actual measured depth. A statistical test was performed to determine differences in the mean creep depth among the composite groups. The dry specimens generally exhibited higher creep behavior— indicating how much the nanoindenter tip penetrated further into the material after initial contact—except for the bulk PFC group (Group 4), which showed a 0.30 ± 0.02 µm versus 0.37 ± 0.01 µm additional creep penetration at 300 s compared to the initial penetration (see Figure 8). The calculated creep depths were also compared using the Bonferroni post hoc test. In the dry specimens, the control group (layered PFC, Group 1) showed a significant difference compared to the layered SFRC (Group 2) specimens ($p < 0.001$), while the layered SFRC (Group 2) also differed significantly from the bulk SFRC (Group 3) ($p < 0.001$) and the bi-structure (Group 5) specimens ($p = 0.024$); furthermore, the bulk SFRC (Group 3) specimens showed a significant difference compared to the bulk PFC specimens (Group 4) ($p = 0.042$). After 30 days of water storage, the control group (layered PFC, Group 1) showed a significant difference compared to all other groups ($p < 0.05$), and the bulk PFC (Group 4) had a significantly greater mean creep depth than the other groups ($p < 0.05$).

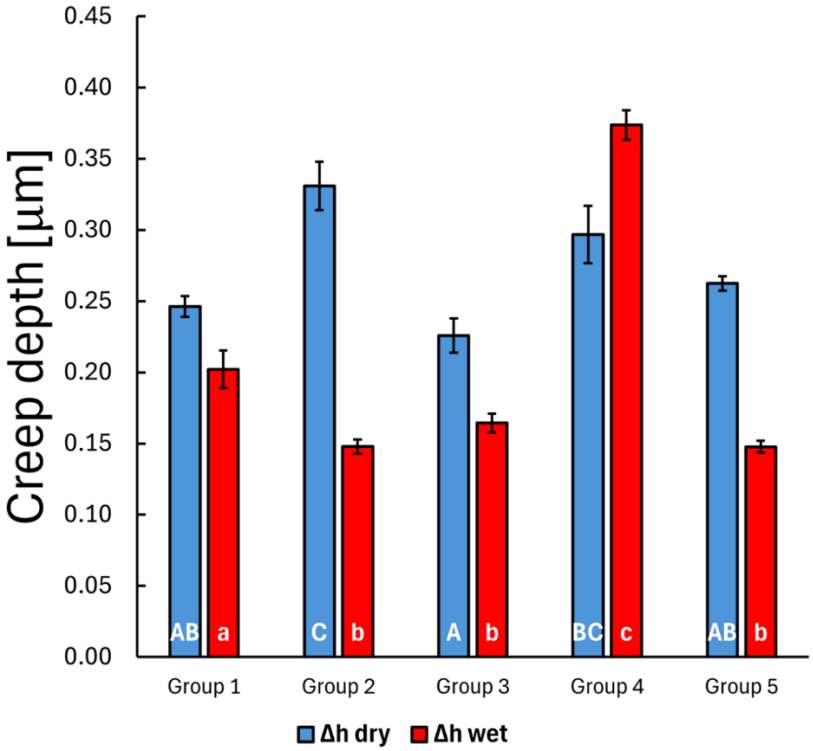

Figure 11. *The mean creep depth at 300 s before and after water treatment. The error bars show the standard error of the mean. Lowercase alphabetic letters (a–c) refer to the dry groups; uppercase alphabetic letters (A–C) refer to the wet groups. Identical letters (regardless of case) indicate no significant difference, whereas different letters (irrespective of case) denote a significant difference.*

5.2.3 Water uptake

The absorbed water mass per unit volume was compared across the groups on day 30. The bulk SFRC specimens (Group 3) differed significantly from all other groups ($p < 0.05$), while the remaining groups showed no statistically significant differences (see Figure 12).

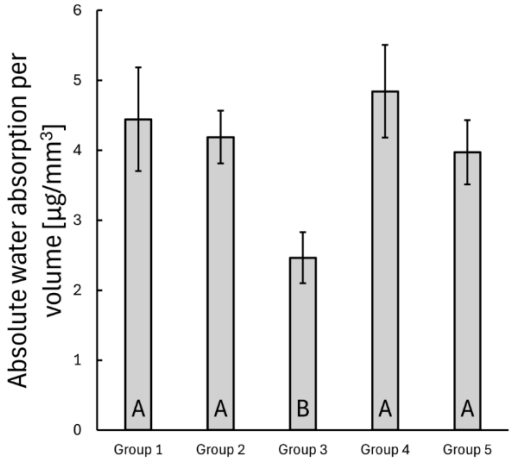

Figure 12. *The mean water absorption per unit volume for each composite group at day 30. The error bars represent the standard error of the mean. Different alphabetic letters indicate statistical significance.*

A linear regression analysis was performed on the absorbed water mass per unit volume dataset, revealing a clear linear trend in water absorption over time. The fitted lines are shown in Figure 13. All groups demonstrated a similar water uptake pattern except for the bulk SFRC (Group 3). A significant correlation was observed, with slopes indicating a daily uptake range between 0.148 and 0.186 µg/mm3, except for the bulk SFRC group (Group 3), where the correlation was weak and the slope was only 0.038 µg/mm3 per day.

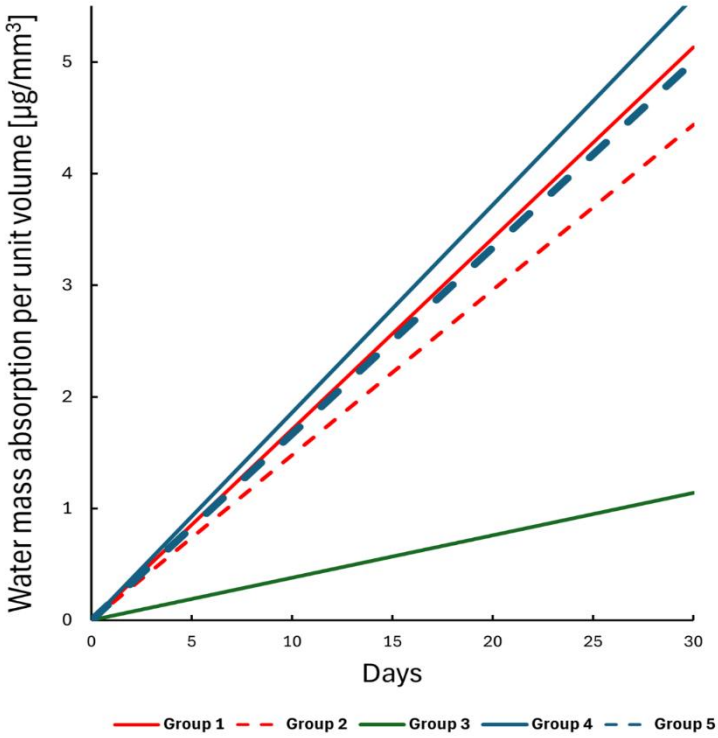

Figure 13. *Linear regression lines for the water mass absorption per unit volume dataset over a 30-day interval.*

5.2.4 SEM evaluation

In Figure 14, the red-marked indentation imprints correspond to the nanoindentation experiments of this study. The dental composite surface exhibited noticeable inhomogeneity at the nanoscale, which partially explains the observed deviations in the mechanical parameters such as hardness and modulus. Notably, no crack propagation was observed in the SEM images, suggesting that the material can accommodate localized deformation without failure (indicating a high fracture toughness).

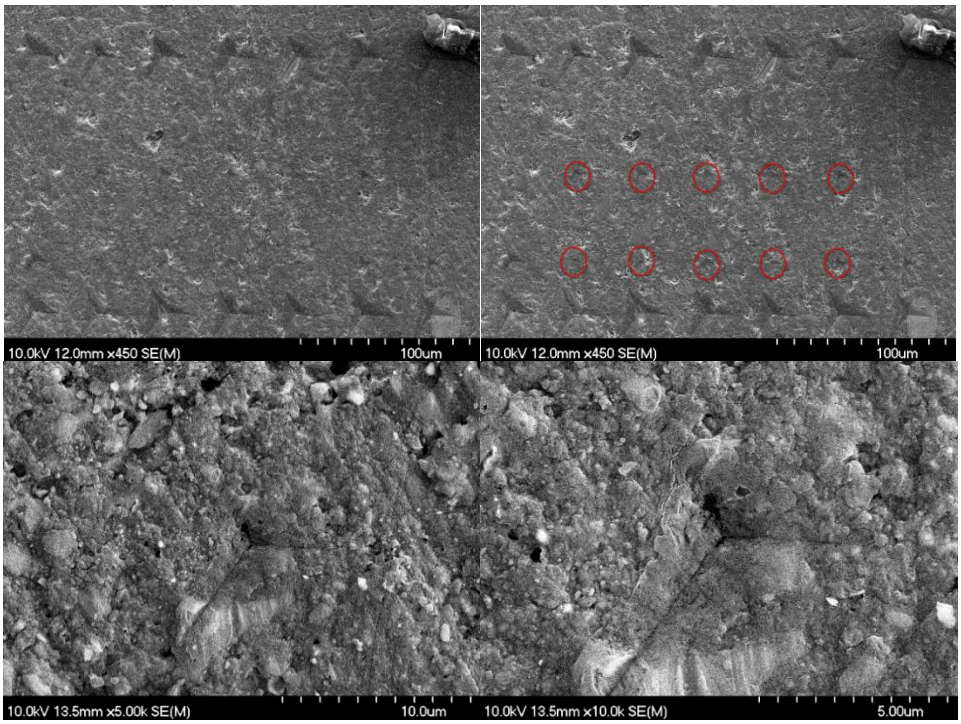

Figure 14. *Scanning electron microscope images of the composite (SDR) specimen surface after nanoindentation at different magnifications. The impressions used in the study are marked in red.*

6. Discussion

Polymerization shrinkage-induced stress in RBC direct restorations remains a clinically relevant problem in dentistry due to its multiple adverse consequences, such as decreased bond strength, gap formation at the margins or between the cavity walls and the filling material, cuspal deformation, and enamel crack development [21,24,113,114]. From the tooth's perspective, cuspal deflection and subsequent enamel crack formation are closely associated with cavity dimensions, particularly the volume factor and the compliance of the cavity walls [56,110,115]. Deep MOD cavities, characterized by the absence of two marginal ridges and a high volume factor, present a unique yet common challenge, both in terms of crack formation [110] and structural reinforcement [108,109,116]. For these reasons, deep MOD cavities with standardized dimensions were selected in our research to analyze crack development during direct restorative techniques performed with different RBC materials.

In our study, when analyzing total crack formation immediately after the restorative procedure, there was no statistically significant difference in the number of cracks among the differently restored groups. Therefore, the first null hypothesis was accepted. This finding is contrary to previous results by Néma et al., in which SFRC-containing direct restorations produced significantly fewer cracks compared to the control group (layered conventional PFC filling)

[110]. Although Soares and colleagues found only a few cracks shorter than 3 mm, the tendency to crack was significantly higher for the direct SFRC group after one week of water storage compared to the indirect and semi-direct groups [100].

However, in the current study, a flowable SFRC was used either alone or in combination with a packable SFRC material, whereas only packable SFRC was utilized in the previous study [100]. In addition, this study employed flowable SFRC without conventional PFC coverage. Typically, neither flowable nor fiber-reinforced RBC materials have been recommended for restoring extensive occlusal hard tissue deficiencies. However, highly filled flowable PFC materials, due to their improved mechanical properties, have been shown to be suitable for both direct [108] and indirect occlusal restorations [116,117].

In their *in vitro* study, Rawda and colleagues reported satisfactory outcomes under clinical conditions where flowable SFRC was used without coverage following an 18-month observation period [118]. Interestingly, neither the conventional flowable PFC base (Group 2) nor the polyethylene fiber mesh combined with the flowable base (Group 3) effectively reduced the number of cracks. This outcome is likely influenced partly by the dimensions of the cavity—and consequently the amount of missing dentin—and partly by the unique characteristics of the flowable SFRC material placed over the aforementioned adhesive bases. The flowable SFRC used in this study (EverX Flow) contains 25 wt% of discontinuous, micrometer-sized fibers with an aspect ratio exceeding 30 [88]. For reinforcement to occur, a fiber's length must meet or exceed the critical fiber length, as discussed earlier in this thesis [86].

To increase the toughness of RBC materials and improve their resistance to damage, polyethylene fibers can be used in addition to short glass fibers [119]. Sadr and colleagues demonstrated that using polyethylene fiber in combination with a conventional flowable PFC as a base resulted in zero polymerization shrinkage-related gap formation in deep cavities [21]. In contrast, our results showed that polyethylene fibers were unable to mitigate cracking more effectively than the flowable SFRC. Furthermore, in our study, the polyethylene fiber was used in combination with SFRC Flow.

When analyzing the total number of cracks one week after the restorative procedure, the control group exhibited a significantly higher number of cracks compared to Group 1 ($p < 0.001$), Group 2 ($p = 0.023$), and Group 3 ($p = 0.003$). Therefore, the second null hypothesis was rejected. These findings align with those of Néma et al. on samples examined after one week [110].

Interestingly, samples restored solely with flowable SFRC (Group 1) exhibited significantly fewer cracks at this time point compared to the mixed use of flowable and paste SFRCs (Group 4) ($p = 0.024$). This difference can likely be attributed to the distinct properties of paste and flowable SFRC materials. While EverX Flow contains a lower quantity of inorganic fillers overall (70 wt%), which results in higher polymerization shrinkage (3.37% for bulk shade and 3.65% for dentin shade, compared to 2.87% for EverX Posterior) [88,120], its proportion of glass fibers is markedly higher (25 wt%) than that in EverX Posterior, which incorporates more inorganic fillers (74.2 wt%) but a relatively smaller amount of glass fibers (9 wt%).

Furthermore, as previously mentioned, the paste variant contains SFRC fibers of millimeter-scale size [121], in contrast to the micrometer-scale fibers of the flowable version [122]. The fine fibers, which undergo full-coverage silane coating, demonstrate enhanced stress absorption and localized load transfer from the matrix to the more robust fibers. In addition to its reduced filler content, the Bis(2-methylpropenoic acid)(1-methylethylidene)bis(4,1-phenyleneoxy-2,1-ethanediyl)ester monomer is a significant contributing factor to the flexibility of EverX Flow. In conjunction with urethane dimethacrylate and triethylene glycol dimethacrylate, it provides fluidity, good handling, and stress relief [123]. To identify the potential causes of the substantial disparities observed in comparison to the control group, it is necessary to consider the impact of the application techniques used. In Groups 1–3, the bulk-fill technique was implemented using flowable RBC, while in Group 4, the bulk-fill technique was employed in conjunction with the snowplow method, utilizing a packable SFRC with a flowable SFRC lining. In the control group (Group 5), layered conventional PFC was applied.

Examining the correlation between internal adaptation, degree of conversion, filling technique, and consistency, a previous study demonstrated that the use of the bulk-fill technique resulted in better internal adaptation after polymerization compared to the application of layered packable RBC [124]. Thus, to some extent, the application technique in the case of non-fiber-reinforced RBC may account for the increased number of cracks detected in this study.

When analyzing the total number of cracks five weeks after the restorative procedure, the same pattern of significant differences among the tested groups was observed as at the one-week time point. Consequently, the third null hypothesis was rejected. Furthermore, when analyzing the total number of cracks within the same group across different time points (immediately after, one week after, and five weeks after the restorative procedure), a significant increase in crack number was observed at each subsequent time point ($p < 0.05$). Therefore, the fourth null

hypothesis was also rejected. It is well recognized that the post-polymerization of RBC materials continues for more than 24 hours after light curing [125] and has even been detected up to one month after curing [126]. Post-polymerization results in an increased degree of conversion [127], which correlates with polymerization shrinkage [120]. Polymerization shrinkage stress causes the cavity walls to deflect in the direction of the restoration [113].

Debonding, defined as the failure of the bond between the RBC and the tooth, may result in the removal of the mechanical constraints acting on the RBC [80]. This, in turn, may lead to the release of residual shrinkage stresses induced by the cavity geometry. Consequently, this process may result in the relaxation of the deformed tooth cusps. Since enamel cracking is linked, to some extent, to the polymerization shrinkage of RBC materials [128], post-cure polymerization likely contributes to the increase in crack numbers observed after restorative treatment [110].

Our results demonstrated a significant increase in the total number of cracks in all groups at both test time points. However, the increase in the number of cracks after five weeks of soaking should most likely not be attributed to post-polymerization and the associated shrinkage stress. As shown in previous research, cuspal flexure has been observed to decrease—or even cease—over time in storage conditions involving water [26]. This process could help neutralize shrinkage-related stresses and thereby close or reduce contraction gaps [80,82,129]. However, it has been noted that the coefficient of hygroscopic expansion of certain restorative materials may exceed that of polymerization shrinkage, which could potentially have undesirable consequences for the remaining tooth structure or the restoration [130,131]. It is possible that internal stresses generated by the expansion of the RBC could result in interfacial strain that exceeds the critical threshold of the dental enamel or of an overlying restoration, leading to the formation of microcracks and subsequent fracture [81,130].

The water uptake of an RBC is predominantly contingent on the chemical nature of the matrix monomers. However, it has been shown that water uptake decreases with an increasing volume fraction of glass fibers [132]. Additionally, the water sorption of barium glass-filled RBCs is relatively high, while the water durability of barium glass is low, resulting in surface degradation of the filler. This, in turn, negatively affects the flexural strength of the material and reduces its resistance to deformation [133].

In the present study, all RBCs contained a high volume fraction of barium glass, except for EverX Flow, in which the barium glass was partially replaced by a relatively high (25%) weight

fraction of glass fibers, thereby contributing to a reduction in water absorption. This aligns with the findings of our second *in vitro* study, which forms the basis of this thesis, showing reduced water uptake in the case of flowable SFRC applied in bulk compared to layered RBC restorations.

When categorizing the total number of cracks into vertical and horizontal types, both showed a significant increase five weeks after the restorative procedure compared to baseline values (immediately after the procedure) in all study groups ($p < 0.05$). When analyzing vertical and horizontal crack counts independently within each group, horizontal cracks consistently predominated over vertical cracks in all SFRC-containing groups (Groups 1–4) at all time points (immediately, one week, and five weeks after the restorative procedure) (Figs. 3 and 4). This is consistent with the findings of Oliveira et al., who also reported a predominance of horizontal post-cure cracks in restored deep MOD cavities [56].

In the control group (layered conventional PFC filling), horizontal cracks were more frequent immediately after and one week after the restorative procedure. However, by five weeks post-intervention, the number of horizontal and vertical cracks was nearly equal (Figs. 3 and 4). This observation may have implications for future crack propagation and potential fracture development.

In our study, direct restorations utilizing flowable SFRC without conventional PFC coverage were evaluated for crack formation. The body of literature on flowable SFRC restorations without conventional PFC coverage is rapidly expanding and shows promising results in terms of mechanical performance [95,99,116,118]. Consequently, it is essential to investigate all associated issues related to this restorative option, such as polymerization stress-induced crack formation. Although enamel cracking is not a direct or reliable measure of shrinkage stress, a correlation can be observed. However, further research is needed to clarify the underlying causes—beyond current hypotheses—of the increased number of cracks observed after extended storage times.

In our investigation of the nanomechanical performance and water uptake of the flowable SFRC material, SFRC was applied using multiple direct restorative techniques. The successful use of dental materials as load-bearing structural components in restored teeth requires adequate mechanical properties. Therefore, the general mechanical characterization of candidate materials is essential. A useful starting point is the measurement of stress–strain (or load–deformation) properties [134]. Nanoindentation allows for the investigation of selected material

properties using small specimen volumes, based on load–displacement data from submicron-scale indentations. It has been proposed as advantageous over conventional methods due to its high force resolution and precise indent positioning [135–137]. In the first part of this study, static nanoindentation was used to evaluate the hardness of different direct restorations at three levels: top, side, and bottom.

The bulk PFC (SDR, Group 4) demonstrated significantly lower hardness values at all three levels compared to the other groups ($p < 0.05$); therefore, the fifth null hypothesis was rejected. These findings align with previous studies, in which bulk PFC (Group 4) exhibited among the lowest surface hardness values of the tested resin composites [138,139]. This difference may be attributed to SDR's lower filler content (68 wt.%) and potentially to a lower degree of monomer conversion and cross-linking compared to the other tested composites [88,140]. On the other hand, SFRC with a 70 wt.% filler loading exhibited comparable or even higher hardness values at the side and bottom levels compared to the control PFC composite group, which had a 77 wt.% filler loading. This can be attributed to the unique structure of flowable SFRC, which, as previously discussed, contains a high proportion of E-glass fibers in addition to barium glass particulate filler. The E-glass fibers, being harder than barium glass particles, likely contribute to the increased hardness observed in the SFRC material. Moreover, the flowable SFRC (bulk shade) is translucent, and its fibers scatter light, which may enhance the degree of conversion.

These findings are consistent with those of Lassila et al., who reported that flowable SFRC demonstrated superior performance across all tested mechanical parameters compared to SDR and some conventional PFCs [88]. Upon examining the bottom part of the specimens, the bulk PFC specimen (Group 4) exhibited significantly lower hardness values than the SFRC groups ($p < 0.001$). This result aligns with the findings of Karacolak et al., who reported that SDR had one of the lowest microhardness values at the bottom of specimens when compared to other bulk-fill materials [141].

Numerous studies have shown a gradual decrease in microhardness values from the top toward the bottom of both conventional and bulk-fill composite materials, with the extent of this decrease varying significantly depending on the type of resin composite [142,143]. Interestingly, no statistically significant difference in hardness at the bottom of the specimens was observed among the other groups. This indicates that flowable SFRC, whether applied in a layered or bulk manner, produced comparable hardness values. These findings align with our

previous study, in which no differences in microhardness values—measured by nanoindentation—were observed between bulk and layered SFRC specimens in artificial root canals [144]. Similarly, our results are consistent with those of Néma et al., who reported no differences in the degree of conversion at different depths (top, middle, bottom) between layered and bulk-fill SFRC restorations [124].

This outcome is likely attributable to the material's translucency and the light transmission facilitated by the short glass fibers [91,117,145,146]. Fráter et al. also demonstrated no difference in fracture resistance between flowable SFRC restorations applied in a layered versus bulk manner [108]. Furthermore, Néma et al. noted no difference in polymerization-induced crack formation between flowable SFRC restorations applied in either technique [110]. However, they also observed that bulk application resulted in less polymerization-induced gap formation compared to the layered application of SFRC material [124].

Notably, after water storage, no difference in hardness was observed between the control group (layered PFC, Group 1) and the bulk PFC (Group 4) specimens. Water can reduce the surface hardness of restorative materials by acting as a plasticizing molecule within the composite matrix. This process softens the polymer resin component by swelling the network and reducing the intermolecular forces between polymeric chains [147,148]. These findings align with reports in the literature indicating that the microhardness of dental composites is higher before water storage than after [149,150]. However, the effect of water on surface microhardness is material-dependent, and not all dental composites show a decrease in hardness after short-term water exposure [151].

As discussed in our previous in vitro study, which forms the basis of this thesis, the polymerization of RBCs continues for up to a month following light curing [126], although most of the conversion occurs within the first 24 hours. Therefore, microhardness was measured one week after fabrication.

In the second phase of the study, creep measurements were conducted. RBCs are polymeric materials with time-dependent mechanical properties [135,152]. The viscoelastic behavior of resin composites represents a critical aspect of their mechanical performance [153,154] and has been widely examined in the literature [43,155–158]. Given the high occlusal loading forces encountered during mastication, viscoelastic properties such as creep strain are important to consider. In clinical scenarios, strain recovery occurs during unloading phases [158]. According to Baroudi et al., composites exhibiting high creep deformation show poor resistance to

mechanical stress, which may adversely affect the long-term durability of restorations [159]. To our knowledge, the creep behavior of flowable SFRC has not been previously tested. In the present study, the bulk application of flowable SFRC (Group 3) demonstrated significantly higher modulus values (E1 and E2) and viscosity (η), as well as better resistance to creep compared to the bulk PFC (SDR, Group 4) ($p < 0.05$), confirming its suitability for use without surface coverage. Therefore, the sixth null hypothesis was rejected.

The incorporation of microfibers into the composite material enhances its modulus and improves both creep and fatigue resistance [28,160]. Creep, as a viscoelastic property, is primarily influenced by filler content—higher filler loading generally leads to reduced creep in these materials [161,162]. However, the extent of creep in resin-based materials also depends on the type and quantity of the resin component, as well as thermal effects that may alter the material's structure [154,163].

According to Watts, creep resistance reflects the viscoelastic stability of a material and its ability to withstand catastrophic failure under load [157]. This observation is consistent with findings on modern SFRC materials, particularly their ability to convert otherwise irreparable failures into repairable ones [29,108,164].

In the study conducted by Molnár et al., fracturegraphy analysis revealed that the primary crack originated from the occlusal surface of the restoration, propagated downward, and extended through the various layers of the restoration and the underlying tooth structure [117]. Several studies have shown that the SFRC substructure provides structural support to composite restorations and acts as a crack prevention layer [102,165,166]. According to Garoushi and colleagues, the thickness of the SFRC substructure plays a critical role, as it influences both the failure mode and the crack-arresting mechanism [122]. Moreover, the thickness of the veneering composite also significantly affects the performance of the restoration.

In this study, the dimensions of deep Class I restorations utilizing flowable SFRC without conventional composite coverage (Groups 2 and 3) were simulated and evaluated using static nanoindentation, nanoindentation creep, and water uptake testing. The authors consider this approach not only novel but also a strength of the study, given the growing body of literature on flowable SFRC restorations without conventional composite coverage, which has demonstrated excellent mechanical performance [29,94,116].

Consequently, it is essential to investigate all surface-related parameters, including bacterial adhesion, gingival irritation, and aesthetic characteristics associated with this restorative option.

In our study, the water uptake of the tested direct resin composite specimens was also evaluated. Bulk SFRC (Group 3) demonstrated significantly lower water absorption compared to the other groups ($p < 0.001$); thus, the seventh null hypothesis was rejected. This result aligns with previous findings in the literature [88].

The water uptake of resin composites is primarily influenced by the hydrophilicity and cross-linking of the polymer network. Additionally, porosity, as well as the nature of the filler and the filler/fiber–matrix interface, contribute to the extent of water uptake during exposure. Interestingly, the bulk application of SFRC showed less water uptake than the layering technique, which may suggest that water diffusion is facilitated by voids or porosity at the interfaces between layers [167]. This can lead to hydrolytic degradation and undesirable anisotropic behavior, potentially compromising the uniformity and mechanical integrity of the restoration [168]. Even though RBCs are widely used in restorative procedures, their compatibility with biological tissues remains a critical consideration, particularly in cases where the materials are in close proximity to soft tissues or exposed to pulpal environments. The biocompatibility of these materials is influenced by factors such as the type and concentration of monomers, the degree of polymerization, and the release of potentially cytotoxic substances during and after curing [169]. Inadequate curing or the presence of residual monomers may lead to adverse cellular responses, including inflammation, cytotoxicity, or reduced cell viability. Therefore, evaluating the tissue response to different composite formulations is essential to ensure their clinical safety and effectiveness.

According to Attik et al., flowable SFRC (EverX Flow) exhibited a less deleterious effect on primary gingival cell viability compared to a bulk-fill PFC (SDR), particularly on day 3 [139]. This trend persisted through day 5, with a noted enhancement in cellular metabolic activity in the presence of SFRC. These findings support the favorable biological response to SFRCs, further endorsing their use in direct restorative dental applications.

The orientation and distribution of fibers in SFRCs play a critical role in determining their mechanical properties and resistance to water sorption. Randomly oriented fibers can provide isotropic reinforcement, offering uniform mechanical strength in all directions, which is particularly advantageous under complex stress conditions. Conversely, a more aligned fiber orientation tends to improve mechanical performance along the primary load-bearing direction, enhancing properties such as flexural strength and fracture toughness [86]. In contrast, uneven or clustered fiber distribution can lead to localized stress concentrations and reduced structural

integrity [160]. Moreover, fiber orientation and packing density influence the composite's porosity and the interfacial bonding between the fibers and the resin matrix—factors that directly affect water sorption. Poorly distributed fibers may create microvoids that facilitate water uptake, potentially accelerating hydrolytic degradation. Thus, optimizing both fiber orientation and distribution is essential for maximizing mechanical performance and minimizing water-related deterioration in short fiber composites.

This study has some limitations. First, the nanoindentation test is highly sensitive and has a narrow measurement range, which could lead to variable results depending on whether the indentation occurs over a fiber or the resin matrix. However, 19 indents were performed per specimen to ensure reliable and representative measurements. Second, solubility was not assessed, which would have provided a broader understanding of the material's degradation behavior. Additionally, different products can vary significantly in terms of fiber or filler type, orientation, distribution, and resin composition—all of which may influence mechanical performance and degradation characteristics.

7. Conclusion and new findings identified based on the results of this research

Within the limitations of these *in vitro* studies and our review, it can be concluded that:

- the bulk application of flowable SFRCs reduces crack formation more effectively than conventional packable PFCs and other tested techniques.
- bulk-applied SFRC exhibited superior mechanical behavior and significantly lower water absorption compared to conventional and bulk-fill PFCs.
- our findings support the use of flowable SFRC (EverX Flow) as a standalone restorative material without the need for covering.
- bulk-applied SFRC showed the most favorable combination of mechanical strength and water resistance among the tested groups

8. Acknowledgments

First and foremost, I am deeply grateful to my supervisor and mentor, Dr. habil. Márk Fráter, for his invaluable support throughout this journey. Beyond his professional guidance, his encouragement and insight were essential to the completion of this thesis. He has been a true inspiration to me, both as a clinician and as a researcher.

I sincerely thank Dr. habil. Edina Lempel for her tremendous support and contribution to the research.

I am also thankful to Dr. Gábor Braunitzer for his valuable assistance with the statistical analysis.

I would like to express my heartfelt thanks to my family—my wife Dorina and our daughter Olívia—for their continuous support, patience, and encouragement.

Finally, I remain eternally grateful to my parents, whose unwavering love, guidance, and example nurtured the ambition that has carried me this far and continues to drive me forward.

9. References

1. Hattab, F.N.; Yassin, O.M. Etiology and Diagnosis of Tooth Wear: A Literature Review and Presentation of Selected Cases. *Int J Prosthodont* **2000**, *13*, 101–107.
2. Crins, L.A.M.J.; Opdam, N.J.M.; Kreulen, C.M.; Bronkhorst, E.M.; Sterenborg, B.A.M.M.; Huysmans, M.C.D.N.J.M.; Loomans, B.A.C. Randomized Controlled Trial on the Performance of Direct and Indirect Composite Restorations in Patients with Severe Tooth Wear. *Dental Materials* **2021**, *37*, 1645–1654, doi:10.1016/j.dental.2021.08.018.
3. Frencken, J.E.; Sharma, P.; Stenhouse, L.; Green, D.; Laverty, D.; Dietrich, T. Global Epidemiology of Dental Caries and Severe Periodontitis – a Comprehensive Review. *J Clinic Periodontology* **2017**, *44*, doi:10.1111/jcpe.12677.
4. Momoi, Y.; Hayashi, M.; Fujitani, M.; Fukushima, M.; Imazato, S.; Kubo, S.; Nikaido, T.; Shimizu, A.; Unemori, M.; Yamaki, C. Clinical Guidelines for Treating Caries in Adults Following a Minimal Intervention Policy—Evidence and Consensus Based Report. *Journal of Dentistry* **2012**, *40*, 95–105, doi:10.1016/j.jdent.2011.10.011.
5. Hurlbutt, M.; Young, D.A. A Best Practices Approach to Caries Management. *Journal of Evidence Based Dental Practice* **2014**, *14*, 77–86, doi:10.1016/j.jebdp.2014.03.006.
6. Barbosa, T.D.S.; Miyakoda, L.S.; Pocztaruk, R.D.L.; Rocha, C.P.; Gavião, M.B.D. Temporomandibular Disorders and Bruxism in Childhood and Adolescence: Review of the Literature. *International Journal of Pediatric Otorhinolaryngology* **2008**, *72*, 299–314, doi:10.1016/j.ijporl.2007.11.006.
7. Lempel, E.; Tóth, Á.; Fábián, T.; Krajczár, K.; Szalma, J. Retrospective Evaluation of Posterior Direct Composite Restorations: 10-Year Findings. *Dental Materials* **2015**, *31*, 115–122, doi:10.1016/j.dental.2014.11.001.
8. Demarco, F.F.; Corrêa, M.B.; Cenci, M.S.; Moraes, R.R.; Opdam, N.J.M. Longevity of Posterior Composite Restorations: Not Only a Matter of Materials. *Dental Materials* **2012**, *28*, 87–101, doi:10.1016/j.dental.2011.09.003.
9. Opdam, N.J.M.; Van De Sande, F.H.; Bronkhorst, E.; Cenci, M.S.; Bottenberg, P.; Pallesen, U.; Gaengler, P.; Lindberg, A.; Huysmans, M.C.D.N.J.M.; Van Dijken, J.W. Longevity of Posterior Composite Restorations: A Systematic Review and Meta-Analysis. *J Dent Res* **2014**, *93*, 943–949, doi:10.1177/0022034514544217.
10. Heintze, S.D.; Rousson, V. Clinical Effectiveness of Direct Class II Restorations - A Meta-Analysis. *The Journal of Adhesive Dentistry* **2012**, *14*, 407–431, doi:10.3290/j.jad.a28390.
11. Heintze, S.D.; Ilie, N.; Hickel, R.; Reis, A.; Loguercio, A.; Rousson, V. Laboratory Mechanical Parameters of Composite Resins and Their Relation to Fractures and Wear in Clinical Trials—A Systematic Review. *Dental Materials* **2017**, *33*, e101–e114, doi:10.1016/j.dental.2016.11.013.
12. Klapdohr, S.; Moszner, N. New Inorganic Components for Dental Filling Composites. *Monatshefte f□r Chemie* **2005**, *136*, 21–45, doi:10.1007/s00706-004-0254-y.
13. *Craig's Restorative Dental Materials*; Sakaguchi, R.L., Powers, J.M., Eds.; 13th ed.; Elsevier/Mosby: St. Louis, Mo, 2012; ISBN 978-0-323-08108-5.
14. Gajewski, V.E.S.; Pfeifer, C.S.; Fróes-Salgado, N.R.G.; Boaro, L.C.C.; Braga, R.R. Monomers Used in Resin Composites: Degree of Conversion, Mechanical Properties and Water Sorption/Solubility. *Braz. Dent. J.* **2012**, *23*, 508–514, doi:10.1590/S0103-64402012000500007.
15. Ferracane, J.L. Resin Composite—State of the Art. *Dental Materials* **2011**, *27*, 29–38, doi:10.1016/j.dental.2010.10.020.
16. Alzraikat, H.; Burrow, M.; Maghaireh, G.; Taha, N. Nanofilled Resin Composite Properties and Clinical Performance: A Review. *Operative Dentistry* **2018**, *43*, E173–E190, doi:10.2341/17-208-T.

17. Magne, P.; Belser, U. *Biomimetic Restorative Dentistry*; Quintessence publishing: Berlin, 2022; ISBN 978-0-86715-572-3.
18. Manhart, J.; Kunzelmann, K.-H.; Chen, H.Y.; Hickel, R. Mechanical Properties and Wear Behavior of Light-Cured Packable Composite Resins. *Dental Materials* **2000**, *16*, 33–40, doi:10.1016/S0109-5641(99)00082-2.
19. Lempel, E.; Szebeni, D.; Őri, Z.; Kiss, T.; Szalma, J.; Lovász, B.V.; Kunsági-Máté, S.; Böddi, K. The Effect of High-Irradiance Rapid Polymerization on Degree of Conversion, Monomer Elution, Polymerization Shrinkage and Porosity of Bulk-Fill Resin Composites. *Dental Materials* **2023**, *39*, 442–453, doi:10.1016/j.dental.2023.03.016.
20. Ohmori, K.; Tasaki, T.; Kimura, S.; Hori, A.; Sakaeda, N.; Hanabusa, M.; Yamamoto, T. Residual Polymerization Stresses in Human Premolars Generated with Class II Composite Restorations. *Journal of the Mechanical Behavior of Biomedical Materials* **2020**, *104*, 103643, doi:10.1016/j.jmbbm.2020.103643.
21. Sadr, A.; Bakhtiari, B.; Hayashi, J.; Luong, M.N.; Chen, Y.-W.; Chyz, G.; Chan, D.; Tagami, J. Effects of Fiber Reinforcement on Adaptation and Bond Strength of a Bulk-Fill Composite in Deep Preparations. *Dental Materials* **2020**, *36*, 527–534, doi:10.1016/j.dental.2020.01.007.
22. Tseng, P.-C.; Chuang, S.-F.; Kaisarly, D.; Kunzelmann, K.-H. Simulating the Shrinkage-Induced Interfacial Damage around Class I Composite Resin Restorations with Damage Mechanics. *Dental Materials* **2023**, *39*, 513–521, doi:10.1016/j.dental.2023.03.020.
23. Tsertsidou, V.; Mourouzis, P.; Dionysopoulos, D.; Pandoleon, P.; Tolidis, K. Fracture Resistance of Class II MOD Cavities Restored by Direct and Indirect Techniques and Different Materials Combination. *Polymers* **2023**, *15*, 3413, doi:10.3390/polym15163413.
24. Soares, C.J.; Faria-E-Silva, A.L.; Rodrigues, M.D.P.; Vilela, A.B.F.; Pfeifer, C.S.; Tantbirojn, D.; Versluis, A. Polymerization Shrinkage Stress of Composite Resins and Resin Cements – What Do We Need to Know? *Braz. oral res.* **2017**, *31*, doi:10.1590/1807-3107bor-2017.vol31.0062.
25. Soares, C.J.; Bicalho, A.A.; Tantbirojn, D.; Versluis, A. Polymerization Shrinkage Stresses in a Premolar Restored with Different Composite Resins and Different Incremental Techniques. *J Adhes Dent* **2013**, *15*, 341–350, doi:10.3290/j.jad.a29012.
26. Versluis, A.; Tantbirojn, D.; Lee, M.S.; Tu, L.S.; DeLong, R. Can Hygroscopic Expansion Compensate Polymerization Shrinkage? Part I. Deformation of Restored Teeth. *Dental Materials* **2011**, *27*, 126–133, doi:10.1016/j.dental.2010.09.007.
27. Lassila, L.; Garoushi, S.; Vallittu, P.K.; Säilynoja, E. Mechanical Properties of Fiber Reinforced Restorative Composite with Two Distinguished Fiber Length Distribution. *Journal of the Mechanical Behavior of Biomedical Materials* **2016**, *60*, 331–338, doi:10.1016/j.jmbbm.2016.01.036.
28. Lassila, L.; Keulemans, F.; Säilynoja, E.; Vallittu, P.K.; Garoushi, S. Mechanical Properties and Fracture Behavior of Flowable Fiber Reinforced Composite Restorations. *Dental Materials* **2018**, *34*, 598–606, doi:10.1016/j.dental.2018.01.002.
29. Garoushi, S.; Sungur, S.; Boz, Y.; Ozkan, P.; Vallittu, P.K.; Uctasli, S.; Lassila, L. Influence of Short-Fiber Composite Base on Fracture Behavior of Direct and Indirect Restorations. *Clin Oral Invest* **2021**, *25*, 4543–4552, doi:10.1007/s00784-020-03768-6.
30. Magne, P.; Oganesyan, T. Premolar Cuspal Flexure as a Function of Restorative Material and Occlusal Contact Location. *Quintessence Int* **2009**, *40*, 363–370.
31. Reeh, E.S.; Messer, H.H.; Douglas, W.H. Reduction in Tooth Stiffness as a Result of Endodontic and Restorative Procedures. *Journal of Endodontics* **1989**, *15*, 512–516, doi:10.1016/S0099-2399(89)80191-8.

32. Manhart, J.; Chen, H.; Hamm, G.; Hickel, R. Buonocore Memorial Lecture. Review of the Clinical Survival of Direct and Indirect Restorations in Posterior Teeth of the Permanent Dentition. *Oper Dent* **2004**, *29*, 481–508.
33. Opdam, N.J.M.; Bronkhorst, E.M.; Roeters, J.M.; Loomans, B.A.C. Longevity and Reasons for Failure of Sandwich and Total-Etch Posterior Composite Resin Restorations. *J Adhes Dent* **2007**, *9*, 469–475.
34. Bernardo, M.; Luis, H.; Martin, M.D.; Leroux, B.G.; Rue, T.; Leitão, J.; DeRouen, T.A. Survival and Reasons for Failure of Amalgam versus Composite Posterior Restorations Placed in a Randomized Clinical Trial. *J Am Dent Assoc* **2007**, *138*, 775–783, doi:10.14219/jada.archive.2007.0265.
35. Reeh, E.S.; Douglas, W.H.; Messer, H.H. Stiffness of Endodontically-Treated Teeth Related to Restoration Technique. *J Dent Res* **1989**, *68*, 1540–1544, doi:10.1177/00220345890680111401.
36. Versluis, A.; Tantbirojn, D. Relationship between Shrinkage and Stress.; 2009.
37. Pereira, R.; Valdívia, A.; Bicalho, A.; Franco, S.; Tantbirojn, D.; Versluis, A.; Soares, C. Effect of Photoactivation Timing on the Mechanical Properties of Resin Cements and Bond Strength of Fiberglass Post to Root Dentin. *Operative Dentistry* **2015**, *40*, E206–E221, doi:10.2341/14-115-L.
38. Bicalho, A.; Pereira, R.; Zanatta, R.; Franco, S.; Tantbirojn, D.; Versluis, A.; Soares, C. Incremental Filling Technique and Composite Material—Part I: Cuspal Deformation, Bond Strength, and Physical Properties. *Operative Dentistry* **2014**, *39*, e71–e82, doi:10.2341/12-441-L.
39. Bicalho, A.; Valdívia, A.; Barreto, B.; Tantbirojn, D.; Versluis, A.; Soares, C. Incremental Filling Technique and Composite Material—Part II: Shrinkage and Shrinkage Stresses. *Operative Dentistry* **2014**, *39*, e83–e92, doi:10.2341/12-442-L.
40. Park, J.; Chang, J.; Ferracane, J.; Lee, I.B. How Should Composite Be Layered to Reduce Shrinkage Stress: Incremental or Bulk Filling? *Dental Materials* **2008**, *24*, 1501–1505, doi:10.1016/j.dental.2008.03.013.
41. Kim, R.J.-Y.; Kim, Y.-J.; Choi, N.-S.; Lee, I.-B. Polymerization Shrinkage, Modulus, and Shrinkage Stress Related to Tooth-Restoration Interfacial Debonding in Bulk-Fill Composites. *Journal of Dentistry* **2015**, *43*, 430–439, doi:10.1016/j.jdent.2015.02.002.
42. Tantbirojn, D.; Versluis, A.; Pintado, M.R.; DeLong, R.; Douglas, W.H. Tooth Deformation Patterns in Molars after Composite Restoration. *Dental Materials* **2004**, *20*, 535–542, doi:10.1016/j.dental.2003.05.008.
43. Braga, R.; Ballester, R.; Ferracane, J. Factors Involved in the Development of Polymerization Shrinkage Stress in Resin-Composites: A Systematic Review. *Dental Materials* **2005**, *21*, 962–970, doi:10.1016/j.dental.2005.04.018.
44. Ellakwa, A.; Cho, N.; Lee, I. The Effect of Resin Matrix Composition on the Polymerization Shrinkage and Rheological Properties of Experimental Dental Composites. *Dental Materials* **2007**, *23*, 1229–1235, doi:10.1016/j.dental.2006.11.004.
45. Kleverlaan, C.J.; Feilzer, A.J. Polymerization Shrinkage and Contraction Stress of Dental Resin Composites. *Dental Materials* **2005**, *21*, 1150–1157, doi:10.1016/j.dental.2005.02.004.
46. Lee, I.B.; Cho, B.H.; Son, H.H.; Um, C.M. A New Method to Measure the Polymerization Shrinkage Kinetics of Light Cured Composites. *J of Oral Rehabilitation* **2005**, *32*, 304–314, doi:10.1111/j.1365-2842.2004.01414.x.
47. Ferracane, J. Developing a More Complete Understanding of Stresses Produced in Dental Composites during Polymerization. *Dental Materials* **2005**, *21*, 36–42, doi:10.1016/j.dental.2004.10.004.

48. Tay, F.R.; Pashley, D.H. Water Treeing--a Potential Mechanism for Degradation of Dentin Adhesives. *Am J Dent* **2003**, *16*, 6–12.
49. Souza-Junior, E.; Souza-Régis, M.; Alonso, R.; Freitas, A.; Sinhoreti, M.; Cunha, L. Effect of the Curing Method and Composite Volume on Marginal and Internal Adaptation of Composite Restoratives. *Operative Dentistry* **2011**, *36*, 231–238, doi:10.2341/10-107-L.
50. Brännström, M. The Hydrodynamic Theory of Dentinal Pain: Sensation in Preparations, Caries, and the Dentinal Crack Syndrome. *Journal of Endodontics* **1986**, *12*, 453–457, doi:10.1016/S0099-2399(86)80198-4.
51. Marzouk, M.A.; Ross, J.A. Cervical Enamel Crazings Associated with Occluso-Proximal Composite Restorations in Posterior Teeth. *Am J Dent* **1989**, *2*, 333–337.
52. Eick, J.D.; Welch, F.H. Polymerization Shrinkage of Posterior Composite Resins and Its Possible Influence on Postoperative Sensitivity. *Quintessence Int* **1986**, *17*, 103–111.
53. Lutz, F.; Krejci, I.; Barbakow, F. Quality and Durability of Marginal Adaptation in Bonded Composite Restorations. *Dental Materials* **1991**, *7*, 107–113, doi:10.1016/0109-5641(91)90055-4.
54. Lee, M.-R.; Cho, B.-H.; Son, H.-H.; Um, C.-M.; Lee, I.-B. Influence of Cavity Dimension and Restoration Methods on the Cusp Deflection of Premolars in Composite Restoration. *Dental Materials* **2007**, *23*, 288–295, doi:10.1016/j.dental.2006.01.025.
55. Jafarpour, S.; El-Badrawy, W.; Jazi, H.; McComb, D. Effect of Composite Insertion Technique on Cuspal Deflection Using an *In vitro* Simulation Model. *Operative Dentistry* **2012**, *37*, 299–305, doi:10.2341/11-086-L.
56. Oliveira, L.R.S.; Braga, S.S.L.; Bicalho, A.A.; Ribeiro, M.T.H.; Price, R.B.; Soares, C.J. Molar Cusp Deformation Evaluated by Micro-CT and Enamel Crack Formation to Compare Incremental and Bulk-Filling Techniques. *Journal of Dentistry* **2018**, *74*, 71–78, doi:10.1016/j.jdent.2018.04.015.
57. Van Heumen, C.C.M.; Tanner, J.; Van Dijken, J.W.V.; Pikaar, R.; Lassila, L.V.J.; Creugers, N.H.J.; Vallittu, P.K.; Kreulen, C.M. Five-Year Survival of 3-Unit Fiber-Reinforced Composite Fixed Partial Dentures in the Posterior Area. *Dental Materials* **2010**, *26*, 954–960, doi:10.1016/j.dental.2010.05.010.
58. Hood, J.A. Biomechanics of the Intact, Prepared and Restored Tooth: Some Clinical Implications. *Int Dent J* **1991**, *41*, 25–32.
59. Meredith, N.; Setchell, D.J. *In vitro* Measurement of Cuspal Strain and Displacement in Composite Restored Teeth. *Journal of Dentistry* **1997**, *25*, 331–337, doi:10.1016/S0300-5712(96)00047-4.
60. Suliman, A.A.; Boyer, D.B.; Lakes, R.S. Interferometric Measurements of Cusp Deformation of Teeth Restored with Composites. *J Dent Res* **1993**, *72*, 1532–1536, doi:10.1177/00220345930720111201.
61. Alomari, Q.D.; Reinhardt, J.W.; Boyer, D.B. Effect of Liners on Cusp Deflection and Gap Formation in Composite Restorations. *Oper Dent* **2001**, *26*, 406–411.
62. Wu, Y.; Cathro, P.; Marino, V. Fracture Resistance and Pattern of the Upper Premolars with Obturated Canals and Restored Endodontic Occlusal Access Cavities. *Journal of Biomedical Research* **2010**, *24*, 474–478, doi:10.1016/S1674-8301(10)60063-2.
63. Versluis, A.; Tantbirojn, D.; Pintado, M.R.; DeLong, R.; Douglas, W.H. Residual Shrinkage Stress Distributions in Molars after Composite Restoration. *Dental Materials* **2004**, *20*, 554–564, doi:10.1016/j.dental.2003.05.007.
64. El-Helali, R.; Dowling, A.H.; McGinley, E.L.; Duncan, H.F.; Fleming, G.J.P. Influence of Resin-Based Composite Restoration Technique and Endodontic Access on Cuspal Deflection and Cervical Microleakage Scores. *Journal of Dentistry* **2013**, *41*, 216–222, doi:10.1016/j.jdent.2012.11.002.

65. Hannig, C.; Westphal, C.; Becker, K.; Attin, T. Fracture Resistance of Endodontically Treated Maxillary Premolars Restored with CAD/CAM Ceramic Inlays. *The Journal of Prosthetic Dentistry* **2005**, *94*, 342–349, doi:10.1016/j.prosdent.2005.08.004.
66. Seo, D.-G.; Yi, Y.-A.; Shin, S.-J.; Park, J.-W. Analysis of Factors Associated with Cracked Teeth. *Journal of Endodontics* **2012**, *38*, 288–292, doi:10.1016/j.joen.2011.11.017.
67. Forster, A.; Braunitzer, G.; Tóth, M.; Szabó, B.P.; Fráter, M. *In vitro* Fracture Resistance of Adhesively Restored Molar Teeth with Different MOD Cavity Dimensions. *Journal of Prosthodontics* **2019**, *28*, doi:10.1111/jopr.12777.
68. Sengupta, A.; Naka, O.; Mehta, S.B.; Banerji, S. The Clinical Performance of Bulk-Fill versus the Incremental Layered Application of Direct Resin Composite Restorations: A Systematic Review. *Evid Based Dent* **2023**, *24*, 143–143, doi:10.1038/s41432-023-00905-4.
69. Unterbrink, G.L.; Liebenberg, W.H. Flowable Resin Composites as "Filled Adhesives": Literature Review and Clinical Recommendations. *Quintessence Int* **1999**, *30*, 249–257.
70. Abbas, G.; Fleming, G.J.P.; Harrington, E.; Shortall, A.C.C.; Burke, F.J.T. Cuspal Movement and Microleakage in Premolar Teeth Restored with a Packable Composite Cured in Bulk or in Increments. *Journal of Dentistry* **2003**, *31*, 437–444, doi:10.1016/S0300-5712(02)00121-5.
71. Versluis, A.; Douglas, W.H.; Cross, M.; Sakaguchi, R.L. Does an Incremental Filling Technique Reduce Polymerization Shrinkage Stresses? *J Dent Res* **1996**, *75*, 871–878, doi:10.1177/00220345960750030301.
72. Rees, J.S.; Jacobsen, P.H. Stresses Generated by Luting Resins during Cementation of Composite and Ceramic Inlays. *J of Oral Rehabilitation* **1992**, *19*, 115–122, doi:10.1111/j.1365-2842.1992.tb01088.x.
73. Davidson, C.L.; de Gee, A.J. Light-Curing Units, Polymerization, and Clinical Implications. *J Adhes Dent* **2000**, *2*, 167–173.
74. Fronza, B.M.; Rueggeberg, F.A.; Braga, R.R.; Mogilevych, B.; Soares, L.E.S.; Martin, A.A.; Ambrosano, G.; Giannini, M. Monomer Conversion, Microhardness, Internal Marginal Adaptation, and Shrinkage Stress of Bulk-Fill Resin Composites. *Dental Materials* **2015**, *31*, 1542–1551, doi:10.1016/j.dental.2015.10.001.
75. Cara, R.R.; Fleming, G.J.P.; Palin, W.M.; Walmsley, A.D.; Burke, F.J.T. Cuspal Deflection and Microleakage in Premolar Teeth Restored with Resin-Based Composites with and without an Intermediary Flowable Layer. *Journal of Dentistry* **2007**, *35*, 482–489, doi:10.1016/j.jdent.2007.01.005.
76. Alhadainy, H.A.; Abdalla, A.I. 2-Year Clinical Evaluation of Dentin Bonding Systems. *Am J Dent* **1996**, *9*, 77–79.
77. Sampaio, P.; De Almeida Júnior, A.; Francisconi, L.; Casas-Apayco, L.; Pereira, J.; Wang, L.; Atta, M. Effect of Conventional and Resin-Modified Glass-Ionomer Liner on Dentin Adhesive Interface of Class I Cavity Walls After Thermocycling. *Operative Dentistry* **2011**, *36*, 403–413, doi:10.2341/09-240-L.
78. Azevedo, L.M.; Casas-Apayco, L.C.; Villavicencio Espinoza, C.A.; Wang, L.; Navarro, M.F.D.L.; Atta, M.T. Effect of Resin-Modified Glass-Ionomer Cement Lining and Composite Layering Technique on the Adhesive Interface of Lateral Wall. *J. Appl. Oral Sci.* **2015**, *23*, 315–320, doi:10.1590/1678-775720140463.
79. Belli, S.; Cobankara, F.K.; Eraslan, O.; Eskitascioglu, G.; Karbhari, V. The Effect of Fiber Insertion on Fracture Resistance of Endodontically Treated Molars with MOD Cavity and Reattached Fractured Lingual Cusps. *J Biomed Mater Res* **2006**, *79B*, 35–41, doi:10.1002/jbm.b.30508.

80. Meriwether, L.A.; Blen, B.J.; Benson, J.H.; Hatch, R.H.; Tantbirojn, D.; Versluis, A. Shrinkage Stress Compensation in Composite-Restored Teeth: Relaxation or Hygroscopic Expansion? *Dental Materials* **2013**, *29*, 573–579, doi:10.1016/j.dental.2013.03.006.
81. Momoi, Y.; McCabe, J.F. Hygroscopic Expansion of Resin Based Composites during 6 Months of Water Storage. *Br Dent J* **1994**, *176*, 91–96, doi:10.1038/sj.bdj.4808379.
82. Suiter, E.A.; Watson, L.E.; Tantbirojn, D.; Lou, J.S.B.; Versluis, A. Effective Expansion: Balance between Shrinkage and Hygroscopic Expansion. *J Dent Res* **2016**, *95*, 543–549, doi:10.1177/0022034516633450.
83. Ruddell, D. Effect of Novel Filler Particles on the Mechanical and Wear Properties of Dental Composites. *Dental Materials* **2002**, *18*, 72–80, doi:10.1016/S0109-5641(01)00022-7.
84. Kim, K. -H.; Okuno, O. Microfracture Behaviour of Composite Resins Containing Irregular-shaped Fillers. *J of Oral Rehabilitation* **2002**, *29*, 1153–1159, doi:10.1046/j.1365-2842.2002.00940.x.
85. Garoushi, S.; Mangoush, E.; Vallittu, M.; Lassila, L. Short Fiber Reinforced Composite: A New Alternative for Direct Onlay Restorations. *TODENTJ* **2013**, *7*, 181–185, doi:10.2174/1874210601307010181.
86. Vallittu, P.K. High-Aspect Ratio Fillers: Fiber-Reinforced Composites and Their Anisotropic Properties. *Dental Materials* **2015**, *31*, 1–7, doi:10.1016/j.dental.2014.07.009.
87. Alshabib, A.; Jurado, C.A.; Tsujimoto, A. Short Fiber-Reinforced Resin-Based Composites (SFRCs); Current Status and Future Perspectives. *Dent. Mater. J.* **2022**, *41*, 647–654, doi:10.4012/dmj.2022-080.
88. Lassila, L.; Keulemans, F.; Vallittu, P.K.; Garoushi, S. Characterization of Restorative Short-Fiber Reinforced Dental Composites. *Dent. Mater. J.* **2020**, *39*, 992–999, doi:10.4012/dmj.2019-088.
89. Dyer, S. Effect of Fiber Position and Orientation on Fracture Load of Fiber-Reinforced Composite. *Dental Materials* **2004**, *20*, 947–955, doi:10.1016/j.dental.2003.12.003.
90. Bijelic-Donova, J.; Garoushi, S.; Lassila, L.V.J.; Keulemans, F.; Vallittu, P.K. Mechanical and Structural Characterization of Discontinuous Fiber-Reinforced Dental Resin Composite. *Journal of Dentistry* **2016**, *52*, 70–78, doi:10.1016/j.jdent.2016.07.009.
91. Garoushi, S.; Säilynoja, E.; Vallittu, P.K.; Lassila, L. Physical Properties and Depth of Cure of a New Short Fiber Reinforced Composite. *Dental Materials* **2013**, *29*, 835–841, doi:10.1016/j.dental.2013.04.016.
92. Wang, L.; Garcia, F.C.P.; De Araújo, P.A.; Franco, E.B.; Mondelli, R.F.L. Wear Resistance of Packable Resin Composites after Simulated Toothbrushing Test. *J Esthet Restor Dent* **2004**, *16*, 303–314, doi:10.1111/j.1708-8240.2004.tb00058.x.
93. Garoushi, S.K.; Hatem, M.; Lassila, L.V.J.; Vallittu, P.K. The Effect of Short Fiber Composite Base on Microleakage and Load-Bearing Capacity of Posterior Restorations. *Acta Biomater Odontol Scand* **2015**, *1*, 6–12, doi:10.3109/23337931.2015.1017576.
94. Garoushi, S.; Akbaşak-Sungur, A.Ö.; Erkut, S.; Vallittu, P.K.; Uctasli, S.; Lassila, L. Evaluation of Fracture Behavior in Short Fiber–Reinforced Direct and Indirect Overlay Restorations. *Clin Oral Invest* **2023**, *27*, 5449–5458, doi:10.1007/s00784-023-05164-2.
95. Lassila, L.; Säilynoja, E.; Prinssi, R.; Vallittu, P.K.; Garoushi, S. Bilayered Composite Restoration: The Effect of Layer Thickness on Fracture Behavior. *Biomaterial Investigations in Dentistry* **2020**, *7*, 80–85, doi:10.1080/26415275.2020.1770094.
96. Garoushi, S.; Vallittu, P.K.; Lassila, L.V.J. Use of Short Fiber-Reinforced Composite with Semi-Interpenetrating Polymer Network Matrix in Fixed Partial Dentures. *J Dent* **2007**, *35*, 403–408, doi:10.1016/j.jdent.2006.11.010.
97. Bijelic-Donova, J.; Garoushi, S.; Vallittu, P.K.; Lassila, L.V.J. Mechanical Properties, Fracture Resistance, and Fatigue Limits of Short Fiber Reinforced Dental Composite Resin.

The Journal of Prosthetic Dentistry **2016**, *115*, 95–102, doi:10.1016/j.prosdent.2015.07.012.
98. Lassila, L.; Haapsaari, A.; Vallittu, P.K.; Garoushi, S. Fracture Resistance of Anterior Crowns Reinforced by Short-Fiber Composite. *Polymers (Basel)* **2022**, *14*, 1809, doi:10.3390/polym14091809.
99. Lassila, L.; Säilynoja, E.; Prinssi, R.; Vallittu, P.K.; Garoushi, S. Fracture Behavior of Bi-Structure Fiber-Reinforced Composite Restorations. *Journal of the Mechanical Behavior of Biomedical Materials* **2020**, *101*, 103444, doi:10.1016/j.jmbbm.2019.103444.
100. Soares, L.M.; Razaghy, M.; Magne, P. Optimization of Large MOD Restorations: Composite Resin Inlays vs. Short Fiber-Reinforced Direct Restorations. *Dental Materials* **2018**, *34*, 587–597, doi:10.1016/j.dental.2018.01.004.
101. Aregawi, W.A.; Fok, A.S.L. Shrinkage Stress and Cuspal Deflection in MOD Restorations: Analytical Solutions and Design Guidelines. *Dental Materials* **2021**, *37*, 783–795, doi:10.1016/j.dental.2021.02.003.
102. Garoushi, S.; Vallittu, P.K.; Lassila, L.V.J. Direct Restoration of Severely Damaged Incisors Using Short Fiber-Reinforced Composite Resin. *Journal of Dentistry* **2007**, *35*, 731–736, doi:10.1016/j.jdent.2007.05.009.
103. Cekic-Nagas, I.; Egilmez, F.; Ergun, G.; Vallittu, P.K.; Lassila, L.V.J. Load-Bearing Capacity of Novel Resin-Based Fixed Dental Prosthesis Materials. *Dental Materials Journal* **2018**, *37*, 49–58, doi:10.4012/dmj.2016-367.
104. Nagata, K.; Garoushi, S.K.; Vallittu, P.K.; Wakabayashi, N.; Takahashi, H.; Lassila, L.V.J. Fracture Behavior of Single-Structure Fiber-Reinforced Composite Restorations. *Acta Biomater Odontol Scand* **2016**, *2*, 118–124, doi:10.1080/23337931.2016.1224670.
105. Keulemans, F.; Lassila, L.V.J.; Garoushi, S.; Vallittu, P.K.; Kleverlaan, C.J.; Feilzer, A.J. The Influence of Framework Design on the Load-Bearing Capacity of Laboratory-Made Inlay-Retained Fibre-Reinforced Composite Fixed Dental Prostheses. *Journal of Biomechanics* **2009**, *42*, 844–849, doi:10.1016/j.jbiomech.2009.01.037.
106. Lassila, L.; Mangoush, E.; Vallittu, P.K.; Garoushi, S. Fracture Behavior of Discontinuous Fiber-Reinforced Composite Inlay-Retained Fixed Partial Denture before and after Fatigue Aging. *J Prosthodont Res* **2023**, *67*, 271–277, doi:10.2186/jpr.jpr_d_22_00050.
107. Bijelic, J.; Garoushi, S.; Vallittu, P.K.; Lassila, L.V.J. Short Fiber Reinforced Composite in Restoring Severely Damaged Incisors. *Acta Odontologica Scandinavica* **2013**, *71*, 1221–1231, doi:10.3109/00016357.2012.757640.
108. Fráter, M.; Sáry, T.; Vincze-Bandi, E.; Volom, A.; Braunitzer, G.; Szabó P., B.; Garoushi, S.; Forster, A. Fracture Behavior of Short Fiber-Reinforced Direct Restorations in Large MOD Cavities. *Polymers* **2021**, *13*, 2040, doi:10.3390/polym13132040.
109. Sáry, T.; Garoushi, S.; Braunitzer, G.; Alleman, D.; Volom, A.; Fráter, M. Fracture Behaviour of MOD Restorations Reinforced by Various Fibre-Reinforced Techniques – An *in vitro* Study. *Journal of the Mechanical Behavior of Biomedical Materials* **2019**, *98*, 348–356, doi:10.1016/j.jmbbm.2019.07.006.
110. Néma, V.; Sáry, T.; Szántó, F.L.; Szabó, B.; Braunitzer, G.; Lassila, L.; Garoushi, S.; Lempel, E.; Fráter, M. Crack Propensity of Different Direct Restorative Procedures in Deep MOD Cavities. *Clin Oral Invest* **2023**, *27*, 2003–2011, doi:10.1007/s00784-023-04927-1.
111. *ISO, ISO 14577-1:2015, Metallic Materials—Instrumented Indentation Test for Hardness and Materials Parameters—Part 1: Test Method, 2015. [Online]. Available: Https://Www.Iso.Org/Standard/56626.Html*;
112. Oliver, W.C.; Pharr, G.M. An Improved Technique for Determining Hardness and Elastic Modulus Using Load and Displacement Sensing Indentation Experiments. *J. Mater. Res.* **1992**, *7*, 1564–1583, doi:10.1557/JMR.1992.1564.

113. Rosatto, C.M.P.; Bicalho, A.A.; Veríssimo, C.; Bragança, G.F.; Rodrigues, M.P.; Tantbirojn, D.; Versluis, A.; Soares, C.J. Mechanical Properties, Shrinkage Stress, Cuspal Strain and Fracture Resistance of Molars Restored with Bulk-Fill Composites and Incremental Filling Technique. *Journal of Dentistry* **2015**, *43*, 1519–1528, doi:10.1016/j.jdent.2015.09.007.
114. Ferracane, J.L.; Hilton, T.J. Polymerization Stress – Is It Clinically Meaningful? *Dental Materials* **2016**, *32*, 1–10, doi:10.1016/j.dental.2015.06.020.
115. Van Dijken, J.W.V.; Pallesen, U. Clinical Performance of a Hybrid Resin Composite with and without an Intermediate Layer of Flowable Resin Composite: A 7-Year Evaluation. *Dental Materials* **2011**, *27*, 150–156, doi:10.1016/j.dental.2010.09.010.
116. Volom, A.; Vincze-Bandi, E.; Sáry, T.; Alleman, D.; Forster, A.; Jakab, A.; Braunitzer, G.; Garoushi, S.; Fráter, M. Fatigue Performance of Endodontically Treated Molars Reinforced with Different Fiber Systems. *Clin Oral Invest* **2023**, *27*, 3211–3220, doi:10.1007/s00784-023-04934-2.
117. Molnár, J.; Fráter, M.; Sáry, T.; Braunitzer, G.; Vallittu, P.K.; Lassila, L.; Garoushi, S. Fatigue Performance of Endodontically Treated Molars Restored with Different Dentin Replacement Materials. *Dental Materials* **2022**, *38*, e83–e93, doi:10.1016/j.dental.2022.02.007.
118. ElAziz, R.H.A.; ElAziz, S.A.A.; ElAziz, P.M.A.; Frater, M.; Vallittu, P.K.; Lassila, L.; Garoushi, S. Clinical Evaluation of Posterior Flowable Short Fiber-Reinforced Composite Restorations without Proximal Surface Coverage. *Odontology* **2024**, *112*, 1274–1283, doi:10.1007/s10266-024-00905-5.
119. Metwaly, A.A.; Elzoghby, A.F.; Abd ElAziz, R.H. Clinical Performance of Polyethylenefiber Reinforced Resin Composite Restorations in Endodontically Treated Teeth: (A Randomized Controlled Clinical Trial). *BMC Oral Health* **2024**, *24*, 1285, doi:10.1186/s12903-024-05009-8.
120. Szczesio-Wlodarczyk, A.; Garoushi, S.; Vallittu, P.; Bociong, K.; Lassila, L. Polymerization Shrinkage of Contemporary Dental Resin Composites: Comparison of Three Measurement Methods with Correlation Analysis. *Journal of the Mechanical Behavior of Biomedical Materials* **2024**, *152*, 106450, doi:10.1016/j.jmbbm.2024.106450.
121. Garoushi, S.; Vallittu, P.; Lassila, L. Mechanical Properties and Radiopacity of Flowable Fiber-Reinforced Composite. *Dent. Mater. J.* **2019**, *38*, 196–202, doi:10.4012/dmj.2018-102.
122. Garoushi, S.; Gargoum, A.; Vallittu, P.K.; Lassila, L. Short Fiber-reinforced Composite Restorations: A Review of the Current Literature. *J of Invest & Clin Dent* **2018**, *9*, e12330, doi:10.1111/jicd.12330.
123. Szczesio-Wlodarczyk, A.; Polikowski, A.; Krasowski, M.; Fronczek, M.; Sokolowski, J.; Bociong, K. The Influence of Low-Molecular-Weight Monomers (TEGDMA, HDDMA, HEMA) on the Properties of Selected Matrices and Composites Based on Bis-GMA and UDMA. *Materials* **2022**, *15*, 2649, doi:10.3390/ma15072649.
124. Néma, V.; Kunsági-Máté, S.; Őri, Z.; Kiss, T.; Szabó, P.; Szalma, J.; Fráter, M.; Lempel, E. Relation between Internal Adaptation and Degree of Conversion of Short-Fiber Reinforced Resin Composites Applied in Bulk or Layered Technique in Deep MOD Cavities. *Dental Materials* **2024**, *40*, 581–592, doi:10.1016/j.dental.2024.02.013.
125. Par, M.; Gamulin, O.; Marovic, D.; Klaric, E.; Tarle, Z. Effect of Temperature on Post-Cure Polymerization of Bulk-Fill Composites. *Journal of Dentistry* **2014**, *42*, 1255–1260, doi:10.1016/j.jdent.2014.08.004.
126. Schneider, L.F.J.; Consani, S.; Ogliari, F.; Correr, A.B.; Sobrinho, L.C.; Sinhoreti, M.A.C. Effect of Time and Polymerization Cycle on the Degree of Conversion of a Resin Composite. *Operative Dentistry* **2006**, *31*, 489–495, doi:10.2341/05-81.

127. Carek, A.; Dukaric, K.; Miler, H.; Marovic, D.; Tarle, Z.; Par, M. Post-Cure Development of the Degree of Conversion and Mechanical Properties of Dual-Curing Resin Cements. *Polymers* **2022**, *14*, 3649, doi:10.3390/polym14173649.
128. Han, L.; Okamoto, A.; Fukushima, M.; Okiji, T. Enamel Micro-Cracks Produced around Restorations with Flowable Composites. *Dental Materials Journal* **2005**, *24*, 83–91, doi:10.4012/dmj.24.83.
129. Huang, C.; Kei, L.; Wei, S.H.Y.; Cheung, G.S.P.; Tay, F.R.; Pashley, D.H. The Influence of Hygroscopic Expansion of Resin-Based Restorative Materials on Artificial Gap Reduction. *J Adhes Dent* **2002**, *4*, 61–71.
130. Sindel, J.; Frankenberger, R.; Krämer, N.; Petschelt, A. Crack Formation of All-Ceramic Crowns Dependent on Different Core Build-up and Luting Materials. *Journal of Dentistry* **1999**, *27*, 175–181, doi:10.1016/S0300-5712(98)00049-9.
131. Kirsten, M.; Matta, R.E.; Belli, R.; Lohbauer, U.; Wichmann, M.; Petschelt, A.; Zorzin, J. Hygroscopic Expansion of Self-Adhesive Resin Cements and the Integrity of All-Ceramic Crowns. *Dental Materials* **2018**, *34*, 1102–1111, doi:10.1016/j.dental.2018.04.008.
132. Lassila, L.V.J.; Nohrström, T.; Vallittu, P.K. The Influence of Short-Term Water Storage on the Flexural Properties of Unidirectional Glass Fiber-Reinforced Composites. *Biomaterials* **2002**, *23*, 2221–2229, doi:10.1016/s0142-9612(01)00355-6.
133. Tarumi, H.; Torii, M.; Tsuchitani, Y. Relationship between Particle Size of Barium Glass Filler and Water Sorption of Light-Cured Composite Resin. *Dental Materials Journal* **1995**, *14*, 37-44,102, doi:10.4012/dmj.14.37.
134. He, L.H.; Swain, M.V. Nanoindentation Derived Stress–Strain Properties of Dental Materials. *Dental Materials* **2007**, *23*, 814–821, doi:10.1016/j.dental.2006.06.017.
135. Sadr, A.; Shimada, Y.; Lu, H.; Tagami, J. The Viscoelastic Behavior of Dental Adhesives: A Nanoindentation Study. *Dental Materials* **2009**, *25*, 13–19, doi:10.1016/j.dental.2008.05.001.
136. Takahashi, A.; Sato, Y.; Uno, S.; Pereira, P.N.R.; Sano, H. Effects of Mechanical Properties of Adhesive Resins on Bond Strength to Dentin. *Dental Materials* **2002**, *18*, 263–268, doi:10.1016/S0109-5641(01)00046-X.
137. Van Meerbeek, B.; Willems, G.; Celis, J.P.; Roos, J.R.; Braem, M.; Lambrechts, P.; Vanherle, G. Assessment by Nano-Indentation of the Hardness and Elasticity of the Resin-Dentin Bonding Area. *J Dent Res* **1993**, *72*, 1434–1442, doi:10.1177/00220345930720101401.
138. ALShaafi, M.M.; Haenel, T.; Sullivan, B.; Labrie, D.; Alqahtani, M.Q.; Price, R.B. Effect of a Broad-Spectrum LED Curing Light on the Knoop Microhardness of Four Posterior Resin Based Composites at 2, 4 and 6-Mm Depths. *Journal of Dentistry* **2016**, *45*, 14–18, doi:10.1016/j.jdent.2015.11.004.
139. Attik, N.; Colon, P.; Gauthier, R.; Chevalier, C.; Grosgogeat, B.; Abouelleil, H. Comparison of Physical and Biological Properties of a Flowable Fiber Reinforced and Bulk Filling Composites. *Dental Materials* **2022**, *38*, e19–e30, doi:10.1016/j.dental.2021.12.029.
140. Harp, Y.S.; Montaser, M.A.; Zaghloul, N.M. Flowable Fiber-Reinforced versus Flowable Bulk-Fill Resin Composites: Degree of Conversion and Microtensile Bond Strength to Dentin in High C-Factor Cavities. *J Esthet Restor Dent* **2022**, *34*, 699–706, doi:10.1111/jerd.12901.
141. Karacolak, G.; Turkun, L.S.; Boyacioglu, H.; Ferracane, J.L. Influence of Increment Thickness on Radiant Energy and Microhardness of Bulk-Fill Resin Composites. *Dental Materials Journal* **2018**, *37*, 206–213, doi:10.4012/dmj.2017-032.

142. Flury, S.; Hayoz, S.; Peutzfeldt, A.; Hüsler, J.; Lussi, A. Depth of Cure of Resin Composites: Is the ISO 4049 Method Suitable for Bulk Fill Materials? *Dental Materials* **2012**, *28*, 521–528, doi:10.1016/j.dental.2012.02.002.
143. Garoushi, S.; Vallittu, P.; Shinya, A.; Lassila, L. Influence of Increment Thickness on Light Transmission, Degree of Conversion and Micro Hardness of Bulk Fill Composites. *Odontology* **2016**, *104*, 291–297, doi:10.1007/s10266-015-0227-0.
144. Fráter, M.; Grosz, J.; Jakab, A.; Braunitzer, G.; Tarjányi, T.; Gulyás, G.; Bali, K.; Villa-Machado, P.A.; Garoushi, S.; Forster, A. Evaluation of Microhardness of Short Fiber-Reinforced Composites inside the Root Canal after Different Light Curing Methods – An *in vitro* Study. *Journal of the Mechanical Behavior of Biomedical Materials* **2024**, *150*, 106324, doi:10.1016/j.jmbbm.2023.106324.
145. Lempel, E.; Őri, Z.; Kincses, D.; Lovász, B.V.; Kunsági-Máté, S.; Szalma, J. Degree of Conversion and *in vitro* Temperature Rise of Pulp Chamber during Polymerization of Flowable and Sculptable Conventional, Bulk-Fill and Short-Fibre Reinforced Resin Composites. *Dental Materials* **2021**, *37*, 983–997, doi:10.1016/j.dental.2021.02.013.
146. Lempel, E.; Őri, Z.; Szalma, J.; Lovász, B.V.; Kiss, A.; Tóth, Á.; Kunsági-Máté, S. Effect of Exposure Time and Pre-Heating on the Conversion Degree of Conventional, Bulk-Fill, Fiber Reinforced and Polyacid-Modified Resin Composites. *Dental Materials* **2019**, *35*, 217–228, doi:10.1016/j.dental.2018.11.017.
147. Alshabib, A.; Silikas, N.; Watts, D.C. Hardness and Fracture Toughness of Resin-Composite Materials with and without Fibers. *Dental Materials* **2019**, *35*, 1194–1203, doi:10.1016/j.dental.2019.05.017.
148. Drummond, J.L. Degradation, Fatigue, and Failure of Resin Dental Composite Materials. *J Dent Res* **2008**, *87*, 710–719, doi:10.1177/154405910808700802.
149. Escamilla-Gómez, G.; Sánchez-Vargas, O.; Escobar-García, D.M.; Pozos-Guillén, A.; Zavala-Alonso, N.V.; Gutiérrez-Sánchez, M.; Pérez-López, J.E.; Sánchez-Balderas, G.; Romo-Ramírez, G.F.; Ortiz-Magdaleno, M. Surface Degradation and Biofilm Formation on Hybrid and Nanohybrid Composites after Immersion in Different Liquids. *J Oral Sci* **2022**, *64*, 263–270, doi:10.2334/josnusd.22-0085.
150. Khairy, N.M.; Elkholany, N.R.; Elembaby, A.E. Evaluation of Surface Microhardness and Gingival Marginal Adaptation of Three Different Bulk-fill Flowable Resin Composites: A Comparative Study. *J Esthet Restor Dent* **2024**, *36*, 920–929, doi:10.1111/jerd.13211.
151. Cavalcante, L.M.; Schneider, L.F.J.; Silikas, N.; Watts, D.C. Surface Integrity of Solvent-Challenged Ormocer-Matrix Composite. *Dental Materials* **2011**, *27*, 173–179, doi:10.1016/j.dental.2010.10.002.
152. Papadogiannis, D.; Tolidis, K.; Gerasimou, P.; Lakes, R.; Papadogiannis, Y. Viscoelastic Properties, Creep Behavior and Degree of Conversion of Bulk Fill Composite Resins. *Dental Materials* **2015**, *31*, 1533–1541, doi:10.1016/j.dental.2015.09.022.
153. Cock, D.J.; Watts, D.C. Time-Dependent Deformation of Composite Restorative Materials in Compression. *J Dent Res* **1985**, *64*, 147–150, doi:10.1177/00220345850640021101.
154. El-Safty, S.; Silikas, N.; Akhtar, R.; Watts, D.C. Nanoindentation Creep versus Bulk Compressive Creep of Dental Resin-Composites. *Dental Materials* **2012**, *28*, 1171–1182, doi:10.1016/j.dental.2012.08.012.
155. El Hejazi, A.A.; Watts, D.C. Creep and Visco-Elastic Recovery of Cured and Secondary-Cured Composites and Resin-Modified Glass-Ionomers. *Dental Materials* **1999**, *15*, 138–143, doi:10.1016/S0109-5641(99)00023-8.
156. Papadogiannis, Y.; Lakes, R.S.; Palaghias, G.; Helvatjoglu-Antoniades, M.; Papadogiannis, D. Fatigue of Packable Dental Composites. *Dental Materials* **2007**, *23*, 235–242, doi:10.1016/j.dental.2006.01.015.

157. Watts, D.C. Elastic Moduli and Visco-Elastic Relaxation. *Journal of Dentistry* **1994**, *22*, 154–158, doi:10.1016/0300-5712(94)90199-6.
158. Kaleem, M.; Masouras, K.; Satterthwaite, J.D.; Silikas, N.; Watts, D.C. Viscoelastic Stability of Resin-Composites under Static and Dynamic Loading. *Dental Materials* **2012**, *28*, e15–e18, doi:10.1016/j.dental.2011.11.026.
159. Baroudi, K.; Silikas, N.; Watts, D.C. Time-dependent Visco-elastic Creep and Recovery of Flowable Composites. *European J Oral Sciences* **2007**, *115*, 517–521, doi:10.1111/j.1600-0722.2007.00487.x.
160. Garoushi, S.; Säilynoja, E.; Frater, M.; Keulemans, F.; Vallittu, P.K.; Lassila, L. A Comparative Evaluation of Commercially Available Short Fiber-Reinforced Composites. *BMC Oral Health* **2024**, *24*, 1573, doi:10.1186/s12903-024-05267-6.
161. Marghalani, H.Y.; Al-jabab, A.S. Compressive Creep and Recovery of Light-Cured Packable Composite Resins. *Dental Materials* **2004**, *20*, 600–610, doi:10.1016/j.dental.2003.10.001.
162. Vaidyanathan, J.; Vaidyanathan, T.K. Flexural Creep Deformation and Recovery in Dental Composites. *Journal of Dentistry* **2001**, *29*, 545–551, doi:10.1016/S0300-5712(01)00049-5.
163. Hirano, S.; Hirasawa, T. Compressive Creep and Recovery of Composite Resins with Various Filler Contents in Water. *Dental Materials Journal* **1992**, *11*, 165-176,218, doi:10.4012/dmj.11.165.
164. Fráter, M.; Forster, A.; Keresztúri, M.; Braunitzer, G.; Nagy, K. *In vitro* Fracture Resistance of Molar Teeth Restored with a Short Fibre-Reinforced Composite Material. *Journal of Dentistry* **2014**, *42*, 1143–1150, doi:10.1016/j.jdent.2014.05.004.
165. Garoushi, S.; Lassila, L.V.J.; Tezvergil, A.; Vallittu, P.K. Static and Fatigue Compression Test for Particulate Filler Composite Resin with Fiber-Reinforced Composite Substructure. *Dental Materials* **2007**, *23*, 17–23, doi:10.1016/j.dental.2005.11.041.
166. Garoushi, S.K.; Lassila, L.V.J.; Vallittu, P.K. Direct Composite Resin Restoration of an Anterior Tooth: Effect of Fiber-Reinforced Composite Substructure. *Eur J Prosthodont Restor Dent* **2007**, *15*, 61–66.
167. Soto-Montero, J.; Giannini, M.; Sebold, M.; de Castro, E.F.; Abreu, J.L.B.; Hirata, R.; Dias, C.T.S.; Price, R.B.T. Comparison of the Operative Time and Presence of Voids of Incremental and Bulk-Filling Techniques on Class II Composite Restorations. *Quintessence Int* **2022**, *53*, 200–208, doi:10.3290/j.qi.b2218737.
168. Curtis, A.R.; Shortall, A.C.; Marquis, P.M.; Palin, W.M. Water Uptake and Strength Characteristics of a Nanofilled Resin-Based Composite. *J Dent* **2008**, *36*, 186–193, doi:10.1016/j.jdent.2007.11.015.
169. Marigo, L.; Triestino, A.; Castagnola, R.; Vincenzoni, F.; Cordaro, M.; Di Stasio, E.; Mordente, A.; Nocca, G. Cytotoxic Evaluation of the New Composite Resin through an Artificial Pulp Chamber. *BioMed Research International* **2022**, *2022*, 5100816, doi:10.1155/2022/5100816.